Horizontally embedded Fe(0) electrocoagulation to enhance As(III) removal in biologically active rapid sand filters for drinking water treatment

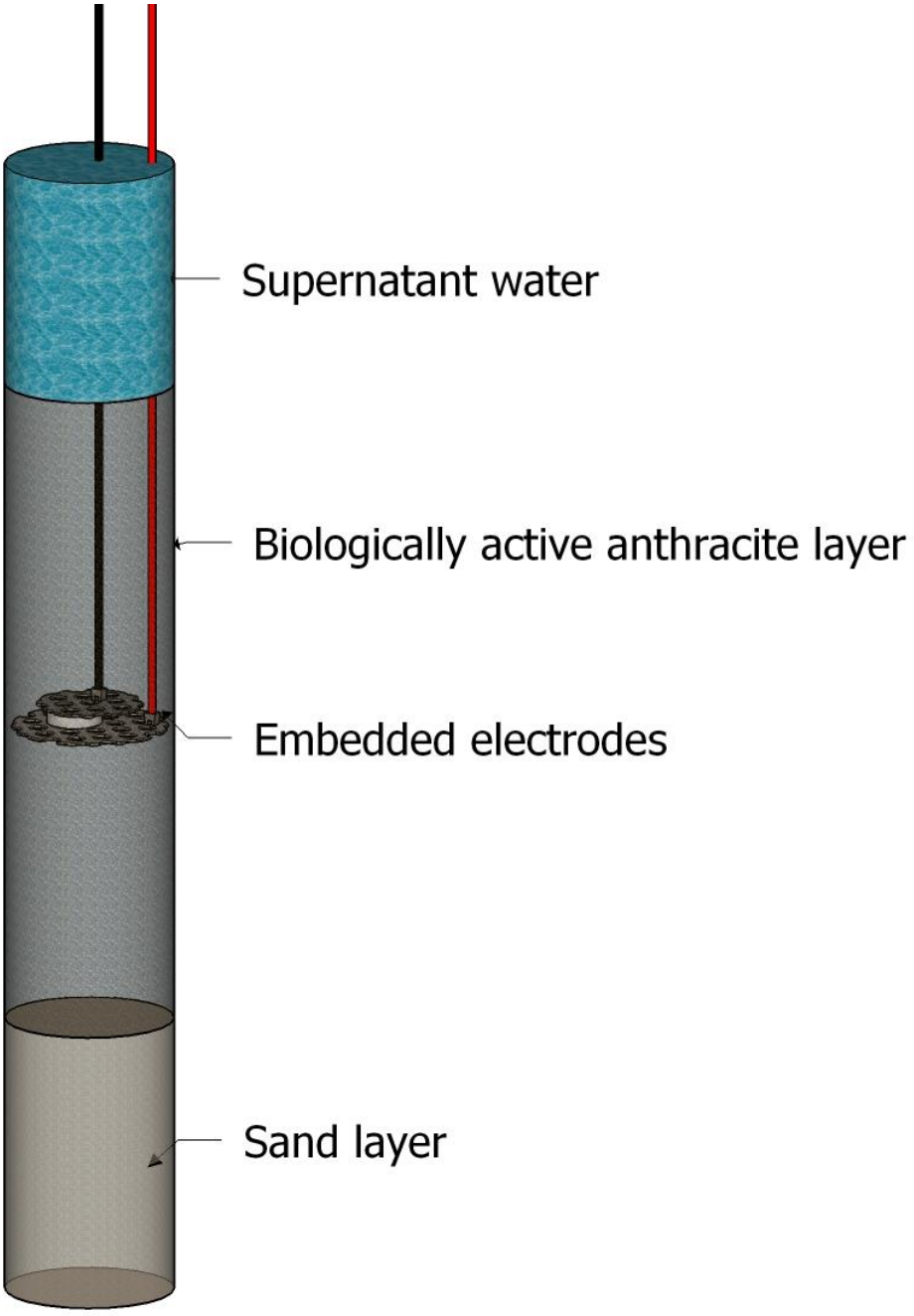

Erik Kraaijeveld

4593294

Master Thesis – August, 2021

Horizontally embedded Fe(0) electrocoagulation to enhance As(III) removal in biologically active rapid sand filters for drinking water treatment

Erik Kraaijeveld
4593294

Delft University of Technology

In partial fulfilment of the requirements for the degree of

Master of Science

in Civil Engineering

To be defended publicly on the 27th of August (2021), at 15:00

Thesis committee:

Chair:	Dr. Ir. D. van Halem	(TU Delft)
First supervisor:	Ir. M. Roy	(TU Delft)
Second supervisor:	Dr. Ir. J.C.J. Gude	(PWN)
External supervisor:	Prof. Dr. Ir. J.B. van Lier	(TU Delft)

TU Delft

Version: - Final thesis - 12-8-2021

Preface and acknowledgements

This work on 'Horizontally embedded Fe(0) electrocoagulation to enhance As(III) removal in biologically active rapid sand filters for drinking water treatment' presents the final thesis of the Master programme (MSc.) Civil Engineering, with a specialization in Water Management (section of Sanitary Engineering), at the Delft University of Technology (TU Delft).

Doing experiments and writing a thesis comes with so called 'ups and downs', where the quality of the report and outcomes of experiments do not always fulfil expectations. Being surrounded by supervisors, colleagues, friends and family with a great work ethic, enthusiasm and passion gave me an incredible boost of motivation to get this work to the level where it is now.

This thesis would not have been possible without the trust, support and guidance I received from my supervisors during the past months. Therefore, I would especially like to thank my daily supervisor Mrinal Roy, who guided me during the experiments in the lab and gave detailed feedback when writing this thesis. It was a real pleasure to work together in the lab in the past months. Not only did he told me everything he knew about arsenic, but I also learned a lot about India and it's culture. Furthermore, I would like to thank Jink Gude for his insights, feedback and our discussions on arsenic removal. Additionally I want to thank Jules van Lier for his feedback and his willingness to be an external supervisor on a short notice. I would like to thank Doris van Halem for her great support during the thinking process and giving the well-needed feedback when writing this thesis. I really appreciated the online 'coffee' hours on Wednesday morning, these provided an interesting discussions and motivation.

Besides my supervisors there are a lot of other people who helped/assisted me during my thesis work. Therefore I have to thank the TU Delft Waterlab staff (Armand, Patricia, Jane and others) and DEMO TUDelft for their support and willingness to help. The drinking water team of Doris (Simon, Bruno, Kajol, and others(!)), thanks all for the valuable feedback and discussion in the weekly 'drinking water meetings' or when answering my (sometimes silly) questions. Also, I want to thank Case van Genuchten for his explanations on electrocoagulation and iron chemistry.

At last I want to thank my dear family and friends for their support, interest and well needed positive distractions during the past months. I apologize for the times my experiments and writing got the priority (also in the evenings) and all the times I 'bored' you with drinking water, sand filters and arsenic removal.

E. Kraaijeveld
Rozenburg, August 2021

Highlights

- Horizontally embedded electrodes in the filter bed resulted in sub-optimal iron utilization for arsenic removal.
- The electrodes in the filter bed resulted in a rapid increase in operational voltage, assumably caused by the accumulation of iron precipitates in the electrochemical cell.
- As(V) experiments showed that the operational performance of the system can be controlled by CD, flowrate and pH.
- Biological arsenic oxidation in RSF is utilized for arsenic removal when placing the Fe-EC electrodes in the supernatant water, improving the arsenic removal.
- Backwashing of the RSF did not affect the biological oxidation of As(III) (by AsOB) in the filter bed significantly.
- Horizontally embedded electrodes within a biologically active filter bed show better arsenic removal compared to electrodes in supernatant, however this required a higher energy input.

Abstract

The aim to reduce arsenic concentrations during groundwater treatment around the world urges the need to develop innovative technologies that can easily be implemented within existing infrastructures and have a high arsenic removal efficiency in terms of low chemical use and energy consumption. This research focussed on fully integrating iron electrocoagulation (Fe-EC) within a biologically active rapid sand filter (RSF) by submerging horizontally perforated electrodes in the filter bed during backwashing. It was hypothesized that the arsenic removal could greatly be enhanced when electrodes were placed in the biologically active filter bed instead of in the supernatant. The arsenic oxidizing bacteria (AsOB) on top of the electrodes oxidized As(III) to As(V), which was then subsequently removed by the iron that got released (by the Fe-EC) and formed precipitates in the filter bed. Iron to arsenic ratios (Fe:As) were reduced from 18.3 to 15.0 when the electrodes were placed in the filter bed instead of in the supernatant (for a charge dosage of 6.4 C/L and 150 µg/L As(III) in the influent), indicating an improved arsenic removal efficiency. As(V) flowthrough experiments showed that the arsenic removal can be improved by lowering the pH from 8 to 7 and by increasing the charge dosage from 6.4 to 9.4 C/L. Iron and As(V) experiments showed the flaws of the integrated system related to a partly homogeneous iron release and improper mixing, resulting in short-circuiting of flows and reduced performance. Further, ways to potentially improve the design of the system are discussed and evaluated, pointing the way forward for future research.

Table of contents

1. Introduction

1.1 Background and urgency

Presence of dissolved arsenic (As) in groundwater, an otherwise preferred drinking water source, has been observed all over the world (Podgorski & Berg, 2020). Chronic exposure to high levels of arsenic, by drinking As-contaminated water, has a major impact on human health. Consumption of As-contaminated water increases the risk of skin, lungs, prostate and kidney cancer, and neurodevelopmental problems in children (Kapaj et al., 2006; Sodhi et al., 2019; Steinmaus et al., 2014). Worldwide, approximately 94 up to 220 million people are exposed to As concentrations exceeding the provisional drinking water guideline of 10 µg/L, set by the World Health Organisation (WHO) (Podgorski & Berg, 2020; WHO, 2004). In Bangladesh and West Bengal (India) over 50 million people are exposed to arsenic concentrations exceeding the WHO guideline and it is estimated that one in five deaths is related to consumption of As-contaminated water (Argos et al., 2010; Kinniburgh & Smedley, 2001).

The 10 µg/L drinking water guideline for arsenic is the first step to ensure a safe drinking water source in the highly affected countries. However, recent studies have shown that the toxicity of arsenic can still cause health-related issues at concentrations below 10 µg/L (Roh et al., 2017; Saint-Jacques et al., 2018). Therefore, most drinking water companies in the Netherlands have adopted the new target of ≤ 1 µg/L as it is considered to be technologically feasible (van der Wens et al., 2016; van Halem et al., 2009). Arsenic concentrations in treated groundwater in the Netherlands are known to reach above the proposed 1 µg/L value, urging the need for technological interventions not only in highly affected countries but also for areas with low arsenic concentrations (Spijker, 2008; Stuijfzand et al., 2008). Therefore it is of upmost importance to implement new technologies to treat As-contaminated water that can easily be integrated within the current infrastructures and supply chains, does not bring significant higher costs, and is capable of reducing As below the desired target concentration (van Genuchten et al., 2020).

1.2 Inefficient arsenic removal by electrocoagulation

Iron Electrocoagulation (Fe-EC), using a sacrificial Fe(0) anode, is a promising electro-chemical Fe-dosage technique to treat As-contaminated (ground)water and has been investigated in a wide range of studies (Flores et al., 2013; Nicomel et al., 2015; Song et al., 2017). Fe-EC has many advantages over the conventional chemical coagulation processes, like the ease of operation and low maintenance, making it a suitable technique for decentralized systems (Song et al., 2017).

Fe-EC systems are driven by a direct current (DC) system with the positive pole connected to the ‘anode’ and the negative pole connected to the ‘cathode’, both placed in the water (bulk solution) (Fig. 1). In Fe-EC, Fe(II) is released from the sacrificial iron anode (eq. 1), which oxidizes and forms ferric

(oxy)hydroxides (HFO) (eq. 2) (Li et al., 2012; Martínez-Villafañe et al., 2009). The formed HFO is known to adsorb, and so remove, the dissolved arsenic present in drinking water sources (Amrose et al., 2013; Goren et al., 2020; van Genuchten et al., 2012). At the cathode (made from iron), reduction of H_2O generates H_2 and OH^- in the bulk solution (eq. 3).

$Fe(s) \rightarrow Fe^{2+}$ (Fe(II)) + 2e (1)

$Fe^{2+} \rightarrow Fe^{3+} + e$ (2)

$Fe^{3+} + 3\ OH^- \rightarrow Fe(OH)_3(s)$ (2)

$Fe^{2+} + 3\ OH^- \rightarrow FeOOH(s) + H_2O + e$ (2)

$2\ H_2O + 2e \rightarrow H_2 + 2\ OH^-$ (3)

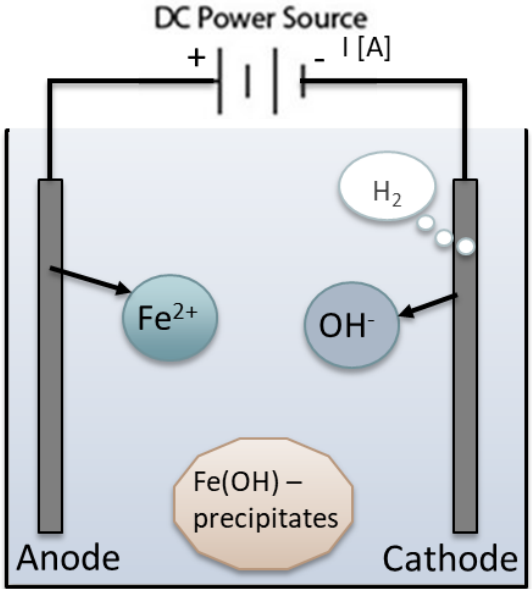

Fig. 1: Schematic overview of Fe-EC processes

The amount of iron that is released by the anode during Fe-EC is proportional to the applied current [A], expressed as Charge Dosage (CD) [C/L] (eq. 4), and can be estimated using Faraday's Law (eq. (5)). The higher the applied current, the more iron will be released.

$$q\ [C/L] = \frac{i * t_{EC}}{V} \quad (4)$$

$$C_{Fe}\ [mg/L] = \frac{q * M_{Fe}}{z_{Fe} * F} = \frac{i * t_{EC} * M_{Fe}}{z_{Fe} * F * V} \quad (5)$$

Where, C_{Fe} = the amount of dissolved iron from the electrode [mg/L]; M_{Fe} = molecular weight of Fe = 55845 mg/mol; i = applied current through DC [A] (=[C/s]); t_{EC} = representative electrolysis time [s]; z_{Fe} = amount of transferred electrons (= 2); F = Faraday's constant = 96485 C/mol; V = solution volume [L].

The arsenic removal efficiency by adsorption to Fe-solids has been proven to be dependent on As oxidation state, where under near-neutral pH conditions (common for groundwater) the affinity of Fe-solids to adsorb the negatively charged arsenate (As(V)) is much higher than that for the neutrally charged arsenite (As(III)) (Bissen & Frimmel, 2003; Dixit & Hering, 2003). Since As(III) is the main arsenic form in raw groundwater, the adsorption of arsenic to Fe-solids can be optimized by oxidizing the As(III) to As(V) prior or during treatment. As(III) could be oxidized to As(V) by O_2 introduced by aeration of the raw groundwater, however this process is slow and takes multiple days. Using chemicals (strong oxidants) to ensure As(III) oxidation prior to treatment would significantly increase the removal efficiency. However, proper handling of chemicals and the formation of toxic by-products are significant drawbacks (Ghurye & Clifford, 2004; Nicomel et al., 2015). A major advantage of Fe-EC operation is the oxidation of As(III) to As(V) by reactive intermediates (ROS) produced during the

oxidation of Fe(II) (Flores et al., 2013; Hug & Leupin, 2003). However, Fe-EC requires a higher iron dosage and so a high energy consumption when aiming to remove As(III) instead of As(V) (Delaire et al., 2017; Wan et al., 2011). Removal of As(V) by Fe-EC can be achieved with an Fe:As ratio (mg/mg) of around 20:1 to 30:1 (Roy et al., 2021; Tong et al., 2014), which is relatively low compared to As(III) removal (100:1 up to 250:1) (Amrose et al., 2013; Kobya et al., 2011, 2016). Expressed in energy consumption, the removal of As(III) requires at least 10 times more energy as the removal of As(V). This implies that the removal of arsenic by Fe-EC can optimized when it is present as As(V) (Goren et al., 2020; Li et al., 2012). As discussed, there are currently no desirable techniques to oxidize the As(III) prior to Fe-EC treatment.

1.3 Limitations of arsenic removal in rapid sand filters

Conventional groundwater treatment plants rely on aeration and rapid sand filtration (RSF), which were designed for the removal of iron, manganese and ammonium (Bruins et al., 2013; Katsoyiannis et al., 2008b). Depending on the iron concentration, arsenic is also partially removed in these passive systems by getting adsorbed on Fe-solids (formed by the oxidation of iron) (Gude, et al., 2018b; Katsoyiannis et al., 2008b). Biological As(III) oxidation over the depth of the filter bed, which can achieved by establishing an As(III) oxidizing microbial community known as arsenic oxidizing bacteria (AsOB), can be considered as a suitable chemical-free oxidation approach (Cavalca et al., 2013; Gude et al., 2018c; Roberts et al., 2004). The advantage of biological oxidation are the low costs involved and the high efficiency of As(III) oxidation without the formation of harmful / toxic by-products (Song et al., 2017). However, relying on biological oxidation in sand filters does not often ensure the desired arsenic removal. The formed iron hydroxides, to which the As(V) will adsorb (Li et al., 2012; van Genuchten et al., 2012), are mostly captured in the top layer of the filter bed (first 10-30 cm) and is therefore not able to adsorb the arsenic that is majorly oxidized after around 40-60 cm (Gude et al., 2018a, 2018b; Yang et al., 2014). This lack of iron (hydroxides) in deeper layers of the filter provokes the reduced arsenic removal during conventional groundwater treatment (Annaduzzaman et al., 2021; Gude, et al., 2018b). Therefore, to reduce the arsenic concentrations in the effluent of the filter, additional Fe dosage is required or As(III) has to be oxidized to As(V) prior to treatment (Gude, et al., 2018b; Roy et al., 2021).

1.4 Research approach

Biological oxidation of As(III) in RSF and As(III) removal by Fe-EC have shown individual advantages over the conventional As(III) oxidation and removal technologies. However they are also associated with individual limitations, such as an additional treatment step required for RSF to effectively remove the oxidized As(V) and the higher iron dosage and energy consumption to remove As(III) by Fe-EC. Combining and integrating biological As(III) oxidation with Fe-EC in a RSF is a promising strategy to exploit their individual advantages and minimize the disadvantages and undesired side effects. It is hypothesised that operating the Fe-EC system within a biologically active RSF bed will be a novel chemical free approach to optimize the As(III) removal in aerated RSF. In a recent study by Roy et al. (2021) it was shown that combining biological As(III) oxidation with Fe-EC in a flowthrough mode removed As(III) more efficient than As(III) alone. However, this configuration of biological As(III) oxidation and Fe-EC has not been investigated as a fully integrated system within a single RSF bed.

During the aforementioned study the filter bed consisted of two separated filter bed layers with the Fe-EC system placed in the water in between these two layers. A fully integrated system would bring major advantages for implementation in the existing treatment infrastructures as no significant modifications of the filter (bed) would be required. Horizontally embedded electrodes (of the Fe-EC system) in the filter bed could provide a homogeneous iron release over the surface of the filter to effectively remove the As(V) after the As(III) is biologically oxidized. This homogeneous iron release would limit the mixing and arsenic removal issues as observed in Gude et al. (2018a), where the iron was introduced chemically in the filter bed of a RSF. Therefore it was proposed to position the Fe-EC system within a RSF below (downstream) a biologically active layer oxidizing As(III), with the anode and cathode (perforated iron plates) being horizontally placed.

To assess the performance of the electrodes in the filter bed in a flowthrough system, it had to be validated whether the release of iron by the Fe-EC integrated in the filter bed was homogeneous over the surface and how mixing improved the uniformity of the iron concentrations. In combination with the comparison of As(V) removal by the integrated electrodes in flowthrough mode against As(V) Fe-EC batch experiments, the arsenic removal efficiency of the electrodes in the filter bed was evaluated. To gain insights in the operational side of the electrodes in the filter bed, As(V) experiments with different operational parameters such as charge dosage (CD), pH and flowrate were performed. The As(III) removal performance of the Fe-EC system was evaluated for a fully integrated system with biological As(III) oxidation upstream of the electrodes and was compared to the experiments with the electrodes in the supernatant (without prior biological oxidation). This would confirm the main hypothesis regarding the enhanced arsenic removal efficiency when placing the electrodes in the filter bed after the biological oxidation. The full performance was evaluated in terms of arsenic oxidation and removal, while considering the energy consumption and rise in supernatant in flowthrough systems.

2. Methodology

2.1 Chemicals and analysis

Dutch tap water (non-chlorinated) was used for all lab experiments (characteristics in Appendix 2). The tap water was spiked with As(III) and As(V) stock solutions to the desired concentration. The stock solutions were prepared by dissolving sodium-(meta)arsenite ($NaAsO_2$) and sodium-arsenate-dibasic-heptahydrate ($Na_2HAsO_4 \bullet 7H_2O$) (Sigma-Aldrich) in Ultra-Pure Water (18.2 mΩ.cm). The stock solutions were freshly prepared every day (or 1 day before) and the As(III) stock solution was acidified to pH 3 using ultrapure HNO_3 acid (ROTIPURAN Ultra 69%) to stop any natural reactions. Further, pH adjustments of the tap water were performed by adding ultrapure HNO_3 acid.

Generally 3 kinds of samples can be distinguished: (a) unfiltered, (b) filtered and (c) resin filtered. Right after collection, the samples were immediately acidified with 1% (v/v) ultrapure HNO_3 to dissolve all solids and stop any further chemical reactions. (a) Unfiltered samples represented the total concentration of ions (dissolved and undissolved) in the bulk solution. These samples were taken and immediately acidified. After 15 minutes, followed by proper shaking, the sample was filtered through a 0.22 µm filter (Macherey-Nagel GmbH & Co. KG) for analysis. (b) Filtered samples represented the dissolved ions in the bulk solution. After taking the water sample, it was immediately filtered through 0.22 µm filters followed by acidification. (c) Resin filtered samples were used for As speciation as they would give the concentration of dissolved As(III). The sample was collected by first filtering it through a 0.22 µm filter followed by passing through an anionic resin (Amberlite IRA-402 resin) using the Clifford method and then acidification (Gude, et al., 2018b). In the Clifford speciation method approx. 14% of the present As(III) would be adsorbed under neutral pH, in this study no corrections have been applied to the measured As(III) concentrations (Gude et al., 2018c). All water samples were collected in triplicates and stored in a dark environment at a temperature of 4 °C prior to analysis. Samples were analysed for As and Fe using Inductively Coupled Plasma Mass Spectrometry (ICP-MS, Analytikal Jena model PlasmaQuant MS ICP-MS).

2.2 Fe-EC batch mode

To quantify the iron release and arsenic removal efficiency of the Fe-EC system, batch experiments with varying operational parameters; CD in range of 5 - 30 C/L and a current of 0.082 A (corresponding to electrolysis time of 1 – 6 minutes), were executed in duplicates (Table 1). The outcome of this experiment resulted in determining the CD to be applied in the flowthrough experiments to remove arsenic concentrations below 10 µg/L.

Table 1: Overview of operating parameters for Fe-EC batch experiments.

CD [C/L]	Applied Current [A]	Electrolysis time [min]	Theoretical Fe [mg/L]
5	0.082	1	1.6
10	0.082	2	3.2
20	0.082	4	6.5
30	0.082	6	9.7

A 1 L glass beaker was filled with 0.9 L tap water and spiked with As(V) to reach 150 µg/L. Perforated electrodes, made of mild steel plates, were horizontally placed in the water and served as the anode and cathode of the Fe-EC system (Appendix 1). The anode was placed on top of the cathode and a plastic spacer was used to maintain a distance of approx. 1.5 cm between the electrodes (Fig. 2). Before the start of the experiment the electrodes were cleaned with sand paper, immersed in a 0.1 M HCl solution for 1 hour and washed with demineralized water to remove any scale and (free) iron precipitates. A magnetic stirrer was set at 120-160 rpm to prevent the settling of the formed iron flocks (on the electrodes or the bottom of the jar) and to ensure uniform mixing of the solution during the experiments and sampling procedures. The initial pH (WTW SenTix 940) and DO (SI Analytics FDO 1100 IDS) of the used tap water (similar to the tap water to be used in flowthrough experiments) was between 7.8-8.0 and 8.3-9.3 mg/L respectively.

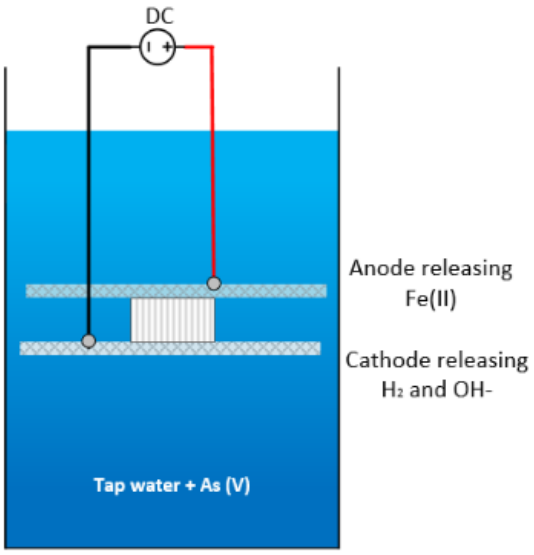

Fig. 2: Schematic overview of Fe-EC batch setup

The extent to which level the amount of iron release corresponds to Faraday's law (eq 5.) is expressed as Faradaic Efficiency (FE) (eq. 6). This equation requires the total amount of iron generated during the experiment and evaluates this value based on the theoretical value from Faraday's law. At the end of the Fe-EC operation, the samples were taken after 5-10 minutes to ensure full oxidation of the released iron. Taking the initial samples before starting the experiments (20 mL total) resulted in a starting volume of 0.88 L, which was used to estimate the Faradaic Efficiency (eq. 5 and 6).

$$FE\ [\%] = \frac{C_{Fe;\ observed}}{C_{Fe;\ theoretical}} * 100\% \quad (6)$$

2.3 Flowthrough experiments

2.3.1 Column design and operation

Flowthrough experiments were performed in down-flow operated PVC columns with a height of 1.7 m and a diameter of 7.5 cm. A total of 4 columns were used, 2 columns for daily experiments with Fe-EC operated within a sand bed and 2 columns to grow the AsOB and investigate the biological oxidation profile of As(III) – As(V). Within the columns for flow through Fe-EC experiments a designated location, consisting of a thin PVC frame, was constructed to ensure the electrodes could be placed horizontally at the desired depth (70 cm above outflow). Inflow of the columns was controlled by multiple feed pumps (Marlow Watson 323), providing the desired flowrate of 3 to 5 m/h. The influent water originated from 20 L drums filled with the relevant water characteristics for the different experiments. The supernatant level was controlled by setting the elevation of the column outflow, and a supernatant level of 20 to 25 cm was maintained above the filter medium. The operational time of the system was dependent on the type of experiment, which relates to the time required to reach system equilibrium/stability. All columns were equipped with backwash facilities that used tap water without air scouring and had sufficient flow to provide the desired 25-30 % bed expansion. Tap water was used for backwashing instead of the filtrate of the column (as done in practice) to ensure the initial state of the column was similar for all days. The column was backwashed at the beginning (15 min) and end of the experiments (till supernatant was visibly clean with an additional 30 min). While backwashing the column at the start of Fe-EC experiments, the electrodes were lowered into the fluidized bed till they were situated horizontally on the supporting frame. After placing the electrodes, the backwashing velocity was slowly reduced and the bed settled. At the end of the experiments, the backwashing was initiated again and the electrodes were removed accordingly.

Before placing the electrodes in the flowthrough experiments, the electrodes were cleaned following the same procedure as for the batch experiments. The anode was placed below the cathode and were kept apart by a plastic spacer (1.5 cm), all tied together by nylon fishing wire to ensure a consistent configuration throughout the experiments (referred to as electrode bundle). This certain anode-cathode configuration was selected to prevent the occurrence of electrical short circuits, caused by the rapid accumulation of iron solids in between the electrodes when the anode would be upstream of the cathode (Mollah et al., 2004). If Iron would be released upstream of the cathode (anode located above the cathode), the high pH near the cathode would cause rapid oxidation resulting in rapid accumulation of iron precipitates in the filter bed near the cathode. This would negatively impact the operation of the sand filter, as rapid localized clogging near the cathode requires more frequent backwashing.

The relevant filter medium of the columns for all experiments was anthracite, which was initially backwashed for 2 hours to ensure it was clean and all fines were removed. For each new set of flowthrough experiments fresh anthracite was used, with an exception for the biologically active

anthracite that was used in the AsOB growth and fully integrated system experiments. The depth of the anthracite layer was dependent on the type of experiments executed and is specified for the range of experiments in the following paragraphs. A dual layer filter, combination of sand and anthracite, was used for the fully integrated experiments to provide the desired filter bed height. Estimations of the characteristics of the sand and anthracite were made. The initial (clean) porosity of the sand and anthracite were estimated at 0.40 and 0.43 (+/- 0.01) respectively. The d_{50}-value of sand and anthracite was estimated at 1.2 and 1.9 mm respectively, based on the particle size distribution (Appendix 3).

2.3.2 Iron release and mixing in the filter bed

To determine the homogeneity of iron release by the horizontally embedded Fe-EC system, iron release experiments were conducted. The CD was set at 6.4 (+/- 0.3) C/L, with the variation caused by the +/- 0.5 L/h deviation in the flowrate and a 1 mA deviation during experiments (Table 2). Three consecutive days of experiments were executed, with 2 duplicate columns operated and sampled each day.

Table 2: Range of operational conditions for iron release experiments

	Values
Current [A]	0.022 - 0.023
Flow [L/h]	12.8 (+/- 0.5)
[m/h]	2.9 (+/- 0.1)
CD [C/L]	6.4 (+/- 0.3)
Theoretical Iron [mg/L]	*1.85 (+/- 0.1)*

The filter bed consisted of 80 cm of anthracite with the electrodes placed at 70 cm from the bottom, with sampling points every 10 cm below the electrodes (Fig. 3). Located 1-2 cm below the anode were the sample points over the surface of the filter bed. These sample points would give insights on the release of iron over the surface of the anode (Fig. 3). To prevent the influence of oxidation and removal of iron in the filter bed, the columns were fed with tap water having pH 4.5 – 5 to hinder iron oxidation. The formation of precipitates in the filter bed would have resulted in inaccurate Faradaic Efficiency (FE) estimations as the iron would be partially retained in the filter bed.

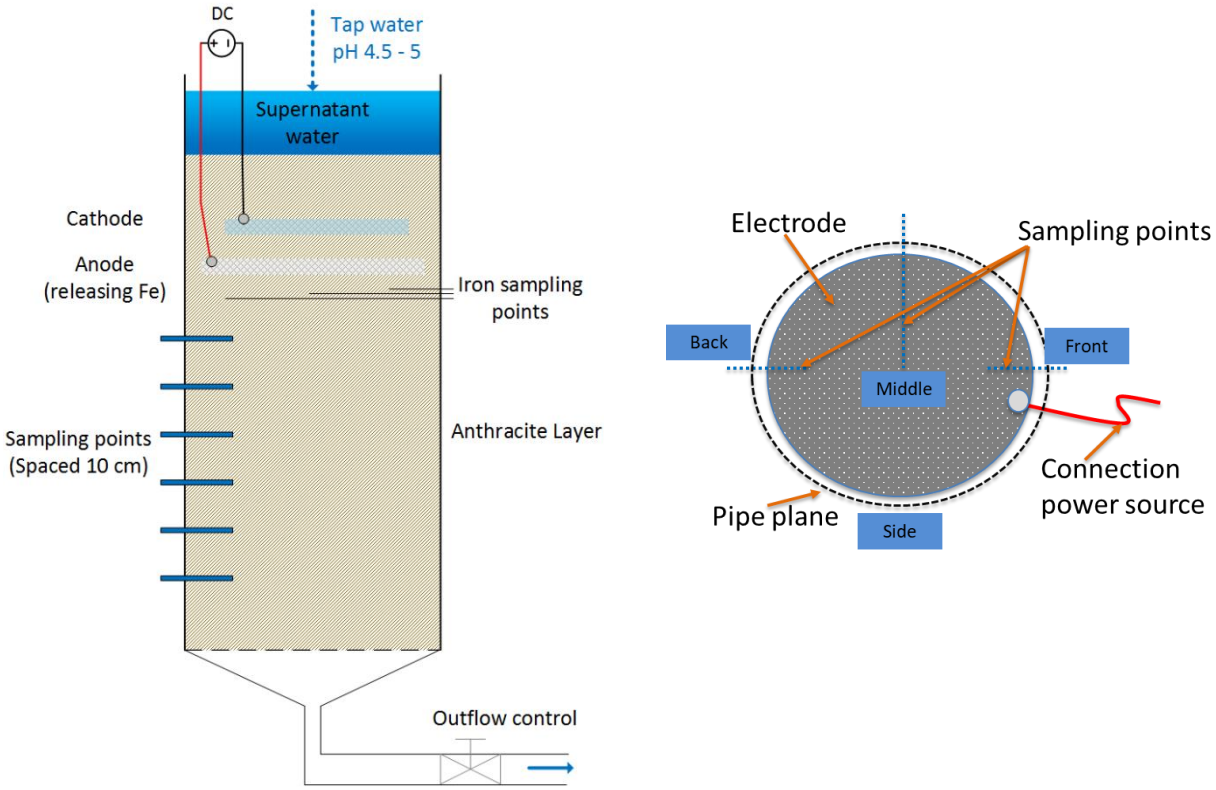

Fig. 3: Schematic overview of experimental setup (left) and sampling points over the surface (right) for the iron release experiments.

The operational procedure shown in Fig. 4 was followed for the experiments. During installation of the electrodes, the location of the connection from the DC power source to the electrodes by the crocodile clamps was reported (as 'Front', 'Back' or 'Side' (Fig. 3)). The operation of the Fe-EC was started once the pH of the effluent reached below 5.0.

The experiments were run for 6 hours, unfiltered samples were taken every 2 hours from the three sampling points over the surface of the filter bed ('Front', 'Middle' and 'Back') and the effluent. Samples (filtered and unfiltered) over the depth and of the effluent were taken at the end of the 6th hour of operation.

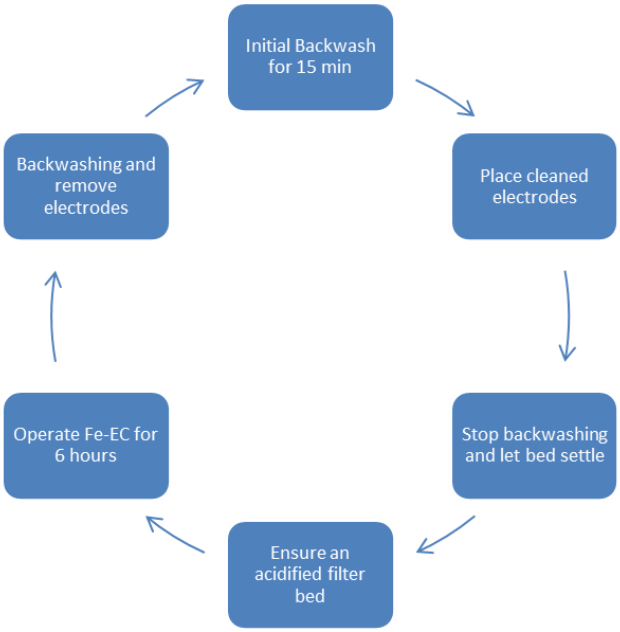

Fig. 4: Overview of experimental procedure for the iron release experiments.

2.3.3 As(V) removal for varying operational conditions with integrated electrodes

Based on the CD required to achieve removal from 150 µg/L As(V) to below the WHO guideline in the Fe-EC in batch experiments, the operational CD for the As(V) flowthrough experiments was set to 6.4 C/L. In addition, experiments were performed with varying operating parameters. For each set of parameters a variable from the reference experiment was changed, resulting in experiments with a higher CD (to 9.4 C/L), higher flowrate (to 5 m/h), and lowered pH (to 7.0) (Table 3).

Table 3: Operational parameters for As(V) flowthrough experiments.

	Reference	**High CD (to 9.4 C/L)**	**High flowrate (to 5 m/h)**	**Low PH (to 7.0)**
Current [A]	0.022	0.033	0.040	0.022
Flow [m/h]	2.9 (+/- 0.1)	2.9 (+/- 0.1)	5.0 (+/- 0.2)	2.9 (+/- 0.1)
CD [C/L]	6.4 (+/- 0.3)	9.4 (+/- 0.3)	6.4 (+/- 0.4)	6.4 (+/- 0.3)
pH	8.0	8.0	8.0	7.0

The filter bed consisted of 85 cm of anthracite with the electrodes placed at 70 cm from the outflow (Fig. 5). The As(V) removal by the electrodes embedded in the filter bed was monitored by following the procedure as in Fig. 5. Two consecutive days of experiments were executed for each of the operating parameters and 2 columns were operated and sampled each day, with an experimental run time of 7 hours. Influent and effluent samples (filtered and unfiltered) were taken hourly from the 4^{th} till the 7^{th} hour of operation to validate whether the column was stable / in equilibrium. After 7 hours of operation samples over the depth of the column were taken (at 10, 30 and 50 cm below the electrodes), followed by the backwashing procedure. During backwashing, 120 mL of backwash water was taken and solids (iron precipitates) were collected by filtering the samples. The solids were stored at -80 °C before being analysed by X-ray adsorption spectroscopy (XAS).

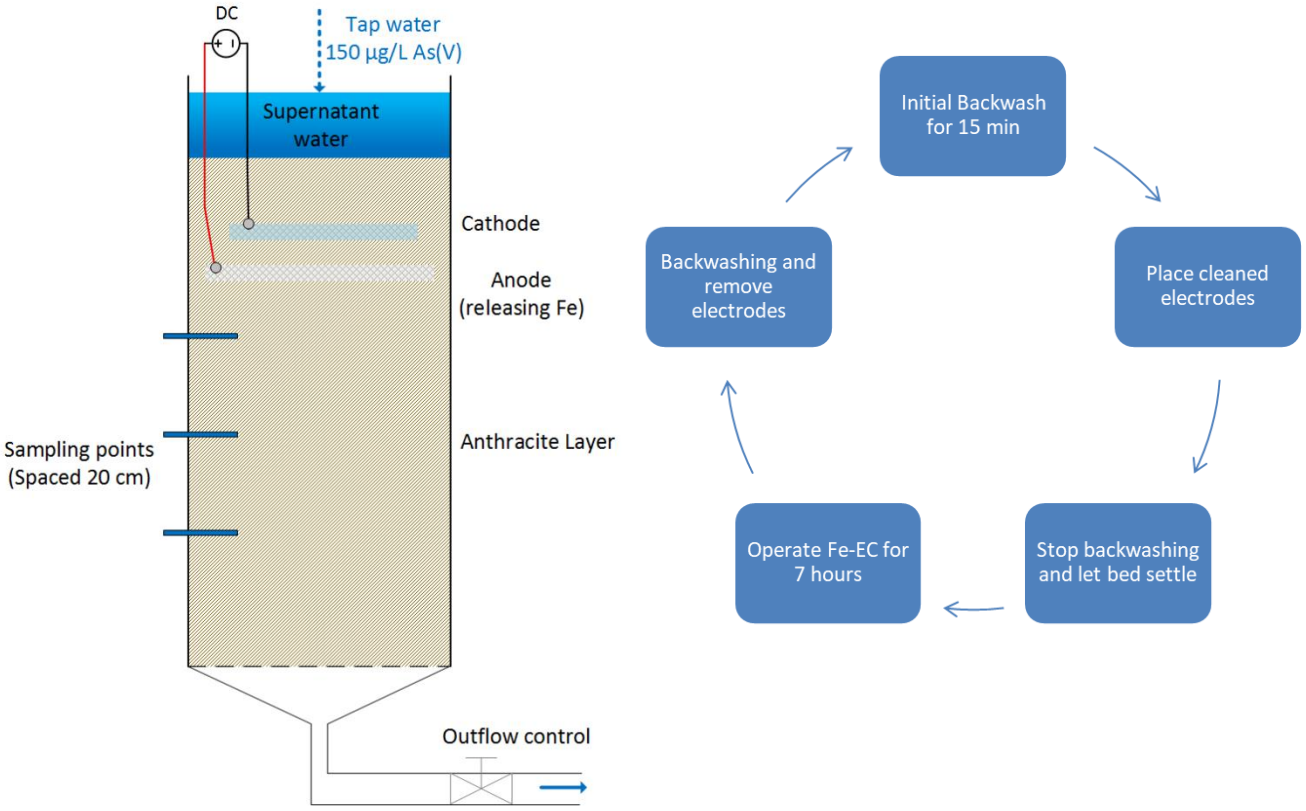

Fig. 5: Schematic overview of the experimental setup (left) and overview of operational procedure (right) for the As(V) flowthrough experiments with the integrated system.

2.3.4 AsOB growth and As(III) oxidation

Continuous down-flow columns, filled with a 80 cm layer of anthracite, were used to establish the AsOB biomass on the anthracite bed that would provide the biological As(III) oxidation in the fully integrated system (Fig. 6). The 2 columns had been wrapped in aluminium foil to provide a realistic filter situation in a dark environment. At the start of the experiment, the column was backwashed for 30 minutes. Then, the column was ripened using tap water spiked with 150 µg/L As(III) at a flowrate of 3 m/h (13.5 L/h) and was running 24/7 for over 60 days. The concentrated As(III) inflow stream (0.3 L/h) combined with a continuously fed tap water flow (13.2 L/h) provided continuous operation during which required the concentrated As(III) jerrycans to be prepared just every 2 to 3 days. This concentrated arsenic stream was acidified to pH 3 - 4 to limit the oxidation of As(III). The pH of the combined influent, at the supernatant, was measured to be around 7.8 (=/- 0.1) during the operational period. The arsenic oxidation was monitored weekly by measuring As(III) concentrations at in- and effluent.

After establishing sufficient AsOB biomass in the column where 95% of the influent As(III) was oxidized in the effluent (after approx. 60 days), an As(III) oxidation profile over the depth was taken. This oxidation profile gave insights into the design of the fully integrated system regarding the thickness of the biological active layer on top of the integrated Fe-EC system. The next step focussed on the effect of backwashing of the biologically active filter bed on the As(III) oxidizing profile. After backwashing, the column was fed with 150 µg/L As(III) and after 5 hours of regular operation (to ensure stability of the column) the oxidation profile over the depth was taken. Differences in the oxidation profile pre and post backwash would be important to consider in the design of the fully integrated system.

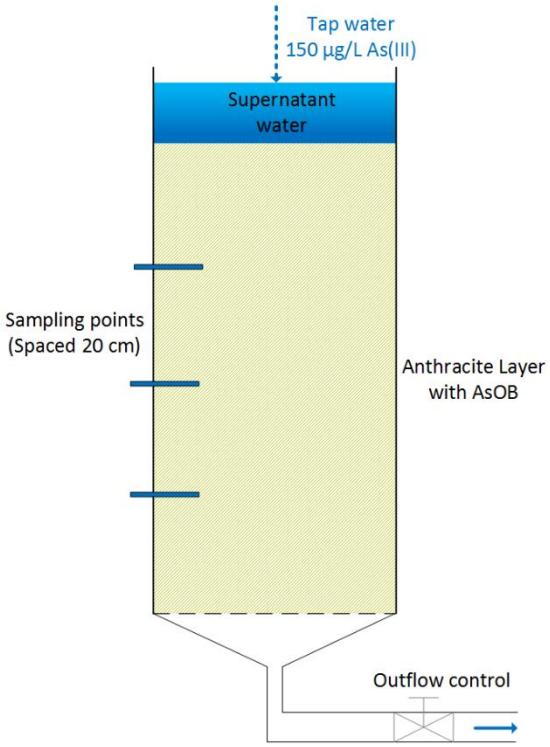

Fig. 6: Schematic overview of the experimental setup for the AsOB growth and oxidation profile experiments.

2.3.5 Fully integrated system

After performing the As(V) batch + flowthrough experiments and establishing the AsOB biomass, the fully integrated setup was assembled. The setup consisted of a 40 cm sand layer at the bottom of the filter with 80 cm of biologically active anthracite on top (representing a small scale dual media filter) and was fed with tap water spiked with 150 µg/L As(III) (Fig. 7). The influent water had a pH of 8.0 (+/- 0.1) and a temperature of 17 (+/- 2) °C. Two electrode configurations were selected: (a) the integrated configuration with the electrodes embedded in the anthracite layer of the filter bed and (b) the reference configuration with the electrodes in the supernatant. The first configuration represented the Fe-EC after biological As(III) oxidation whereas the second one presented the Fe-EC without prior biological As(III) oxidation. In the first configuration the electrodes were located at 70 cm above the outflow point, with a total of 50 cm of biologically active anthracite on top of the electrode (total bed height of 120 cm). In the second configuration the electrodes were located 135

cm above the outflow point, as the total filter bed height was 120 cm the electrodes were located in the supernatant 15 cm above the filter bed.

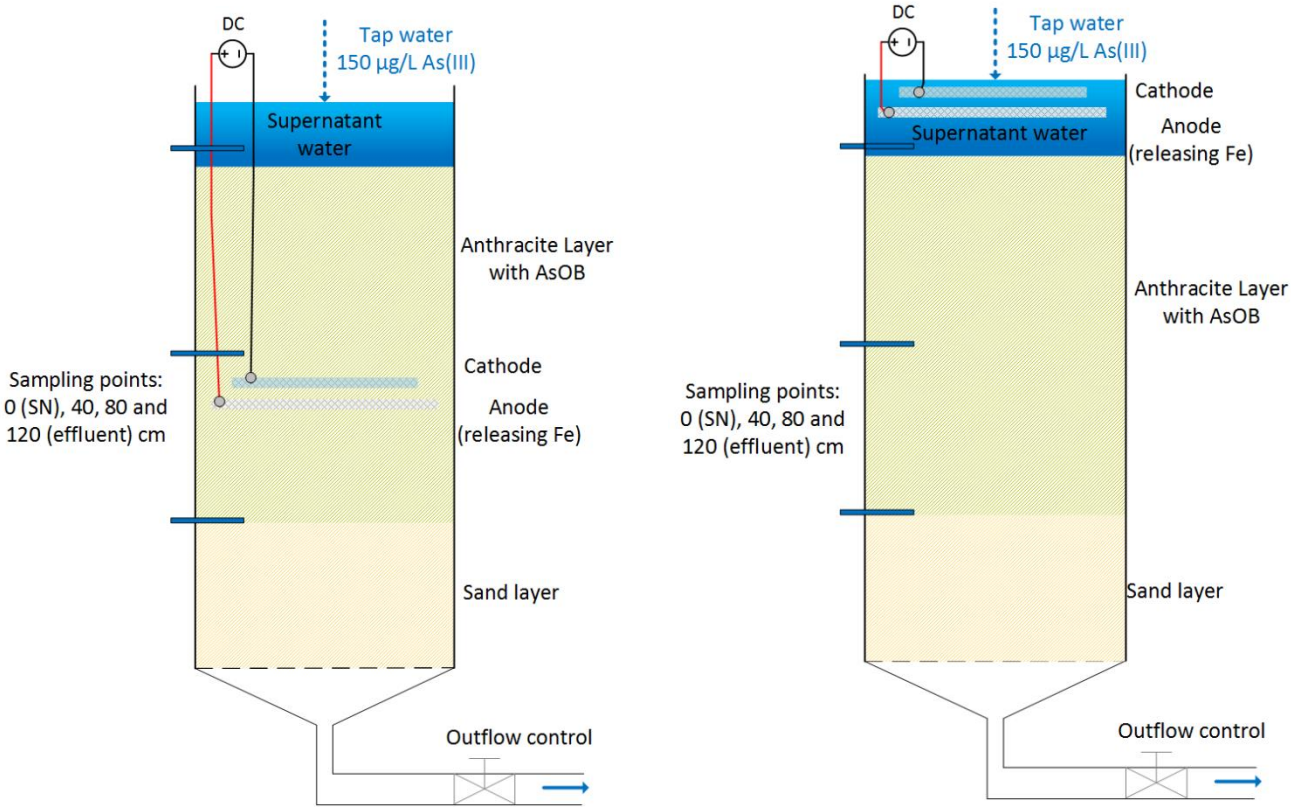

Fig. 7: Schematic overview of the experimental setups for the fully integrated experiments. With the fully integrated system with electrodes embedded in the filter bed (left) and the electrodes in the supernatant water (right).

Similar to the previous experiments, the CD was set at 6.4 C/L so that the results could be compared against As(V) experiments and the performance of the Fe-EC system and biological oxidation could be distinguished (Table 4) .

Table 4: Operating parameters for fully integrated experiments using AsOB and Fe-EC.

	Integrated system	**Reference system**
Electrode location	Integrated in filter bed	In supernatant
Current [A]	0.023	
Flow [m/h]	2.9 (+/- 0.1)	
CD [C/L]	6.4 (+/- 0.3)	

Three consecutive days of experiments were executed, with 2 columns operated and sampled each day. The Fe-EC was operated for a total of 11 hours, starting with an initial backwash followed by continuous operation to ensure stability of the column when sampling (Fig. 8). Influent and effluent arsenic concentrations were sampled at the 7^{th}, 9^{th} and 11^{th} hour of operation to confirm stability of the column. At the end of operation (11^{th} hour), the column was sampled over the depth at the relevant sampling points to obtain the arsenic and iron oxidation/removal profile (Fig. 7). Similar to the As(V)

experiments, solids of the backwash water were also collected for XAS characterisation. To prevent the effects of desorption of the arsenic from the filter material (sand and anthracite), the columns were operated with tap water (not spiked with As) for 12 hours prior to the start of the experiments for each day.

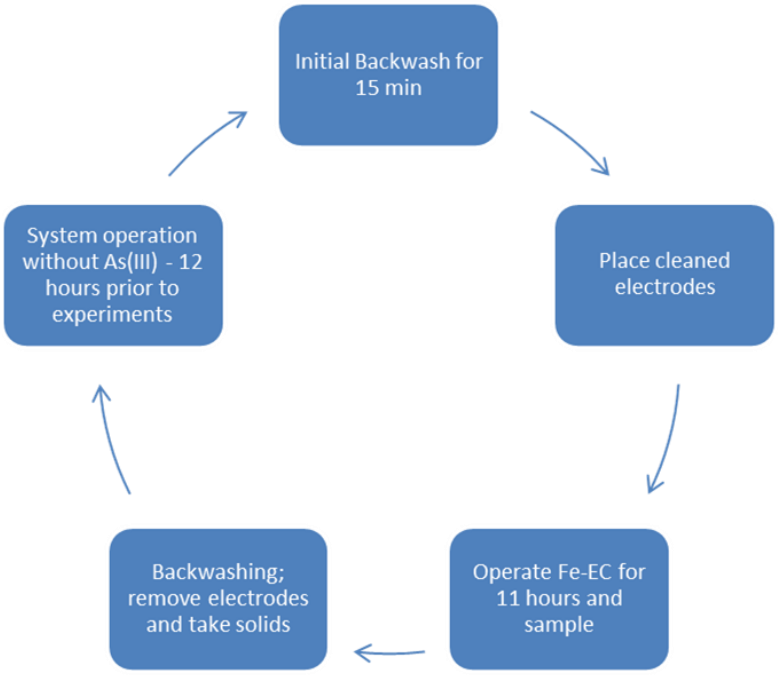

Fig. 8: Overview of experimental procedure for the fully integrated experiments.

3. Results

3.1 Operational parameter estimations by batch Fe-EC experiments

To quantify the charge dosage (with corresponding iron dosage) required in the flowthrough systems to remove 150 µg/L below 10 µg/L (and < 1 µg/L), batch Fe-EC experiments on As(V) removal were executed for a range of CDs with a CDR of 5 C/L/min (corresponding to i = 0.083 A). Fig. 9 shows that with an increase in CD, and corresponding increase in released iron, the As(V) removal increased which is similar to other Fe-EC batch studies where As(V) was removed (Roy et al., 2021; Tong et al., 2014). Measurements of the total iron generated during the batch experiments revealed a Faradaic Efficiency of 0.95 up to 1, which is in line with literature (van Genuchten et al., 2017, 2018). Further, all released Fe(II) was oxidized in the 5 to 10 minutes after electrolysis time, as no residual iron could be found in filtered samples at the end of the experiments.

With a CD of 7.1 C/L (2.1 mg/L of Fe), the initial 150 µg/L As(V) was successfully reduced below the WHO guideline of 10 µg/L. Further, with CD values over 23 C/L (6.6 mg/L of Fe), As(V) was removed to concentrations below 1 µg/L. Fe:As ratio (mg:mg) of 15 and 45 were found to achieve arsenic concentrations of 10 and 1 µg/L respectively (corresponding CD of 7 and 23 C/L), matching previously found Fe:As(V) ratios (Roy et al., 2021; Tong et al., 2014). From these data it was assumed that a CD of approx. 6.4 C/L would be sufficient to remove 150 µg/L As(V) below the WHO guideline, which corresponds to an iron dosage of 1.85 mg/L and an Fe:As ratio of approx. 13.2.

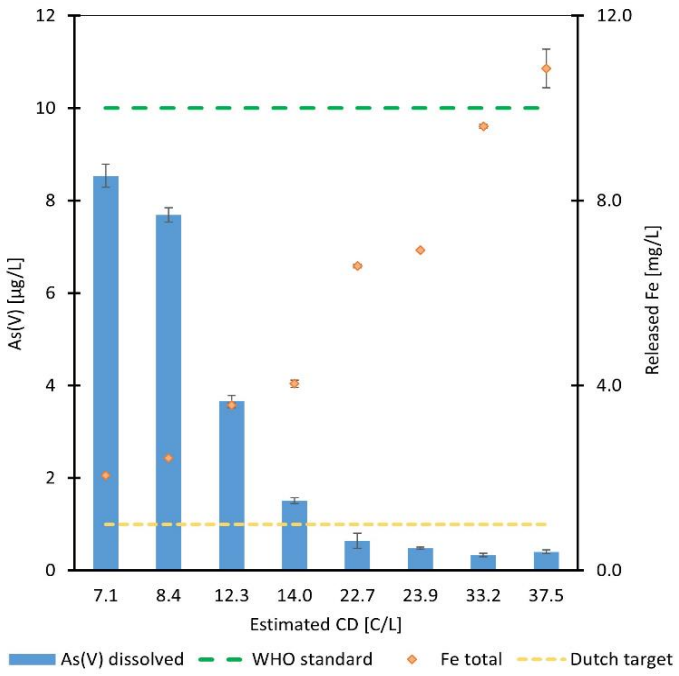

Fig. 9: As(V) removal and iron generation for batch experiments with varying CD. Final dissolved arsenic concentrations are presented and all experiments had an initial dissolved As(V) concentration of 150 (+/- 5) µg/L.

3.2 Homogeneity of iron release by Fe-EC embedded in the filter bed

A CD of 6.4 (+/- 0.3) C/L was selected for the iron release experiments, based on the experimental results in paragraph 3.1. The iron concentrations in the effluent varied between 1.7 and 2.1 mg/L for all experiments (Fig. 10), with the deviation caused by variations in applied CD (+/- 0.3 C/L). Effluent iron concentrations approx. matched the estimations by Faraday's law with a FE of 95 – 105%. These 5% deviations could be caused by the fluctuations in flowrate (+/- 0.1 m/h), resulting in an inaccurate theoretical iron estimation.

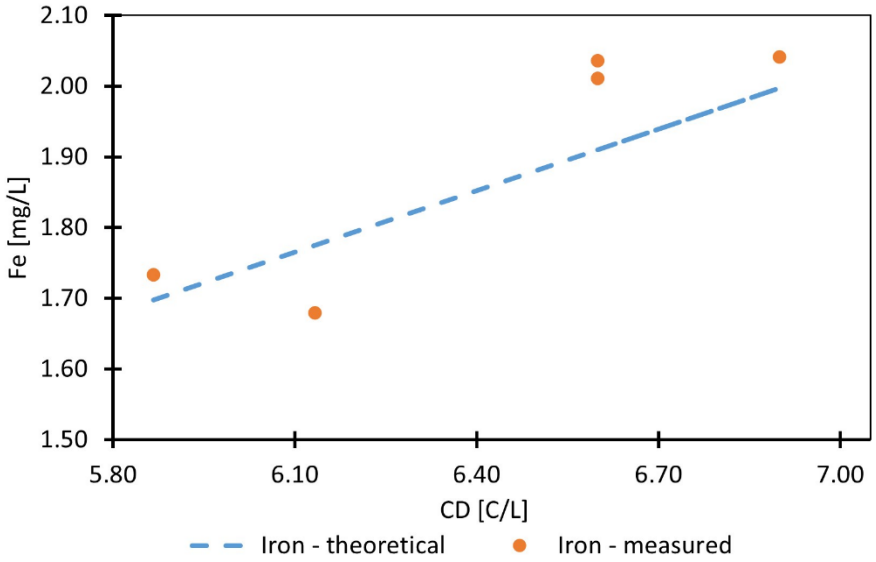

Fig. 10: Effluent Fe concentration vs. theoretical iron concentrations by Faraday's law for a range of CDs with the system operated at a pH of 5.

Samples taken at the sample points (Front, Middle and Back) over the surface plane of the filter bed (Fig. 3) revealed variations in iron concentration between 1 and 4 mg/L, suggesting the iron release by the anode was not fully homogeneous. At 10 cm below the anode iron concentrations deviated between 1 to 4 mg/L for the different experiments sampled at the sampling points over the depth (Fig. 11). This deviation is in line with the aforementioned range of iron concentrations when sampling over the surface of the filter bed (1-2 cm below the anode). As discussed earlier, iron concentrations in the effluent of the column approximately matched the Faradaic estimations. Over the depth of the columns the deviation in iron concentrations decreased from 1-4 mg/L near the anodes to 1.7-2.0 mg/L in the effluent. Lowering the pH to 5 successfully prevented the oxidation and subsequent removal of the iron released in the filter bed, as the effluent iron concentrations did not show a FE significantly smaller than 1 ($p>0.05$ in one-way Anova analysis) which would be expected when iron was removed in the filter bed. This implies that the depth profiles of the column shows mixing of iron in the filter bed (Fig. 11). To achieve uniform iron concentrations approx. 60 to 70 cm of filter bed is needed to ensure proper mixing of the iron with the bulk solution.

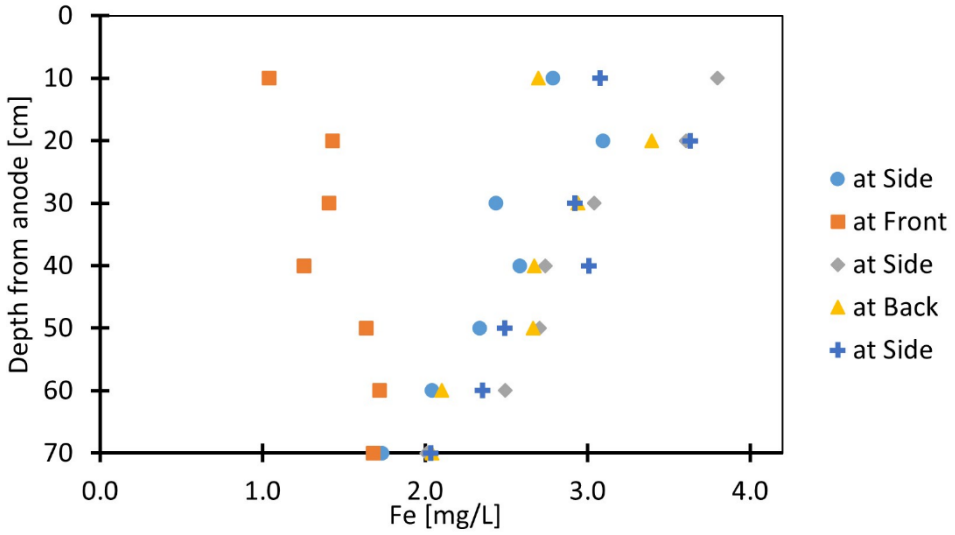

Fig. 11: Depth profile of Fe at the 7th hour of the experiments. The data has been labelled as the location of where the electrode was connected (Fig. 3).

3.3 Effect of operating conditions on As(V) removal by Fe-EC embedded in the filter bed

3.3.1 Increasing CD from 6.4 to 9.4 C/L

Fig. 12 shows the removal of As and Fe over the depth of the duplicate flowthrough columns at the end of operation (7th hour) as an average of the three days of operation. Iron was released by operating the electrodes, embedded in the filter bed, at 6.4 C/L. The influent 150 (+/- 5) µg/L As(V) got reduced to 39 µg/L in the effluent. Of this 39 µg/L effluent As(V), 18 µg/L was As(V) that had been adsorbed to HFO flocks, which did not get removed by the anthracite filter bed, and the rest (21 µg/L) was dissolved As(V). With a finer filter material or a thicker filter layer these particulate HFO flocks (with adsorbed arsenic) would be removed by the filter, potentially resulting in an effluent arsenic concentration of 21 µg/L. Considering the dissolved arsenic concentration in the effluent, the Fe:As ratio was around 14.3 and 86% of the influent As(V) was removed. With 1.85 mg/L of iron released at the anode, 1.72 mg/L (92%) of the released iron had been oxidized at 10 cm below the anode. In this 10 cm filtration, roughly 0.86 mg/L (50 %) of the total released iron was already removed by the filter. After 60 cm of additional filtration, with an estimated residence time of 12 minutes, over 97% of the iron was oxidized and 80% of the iron was removed. At the end of the 7th hour of operation, the iron retention in the filter bed had caused a supernatant rise of + 1.5 cm.

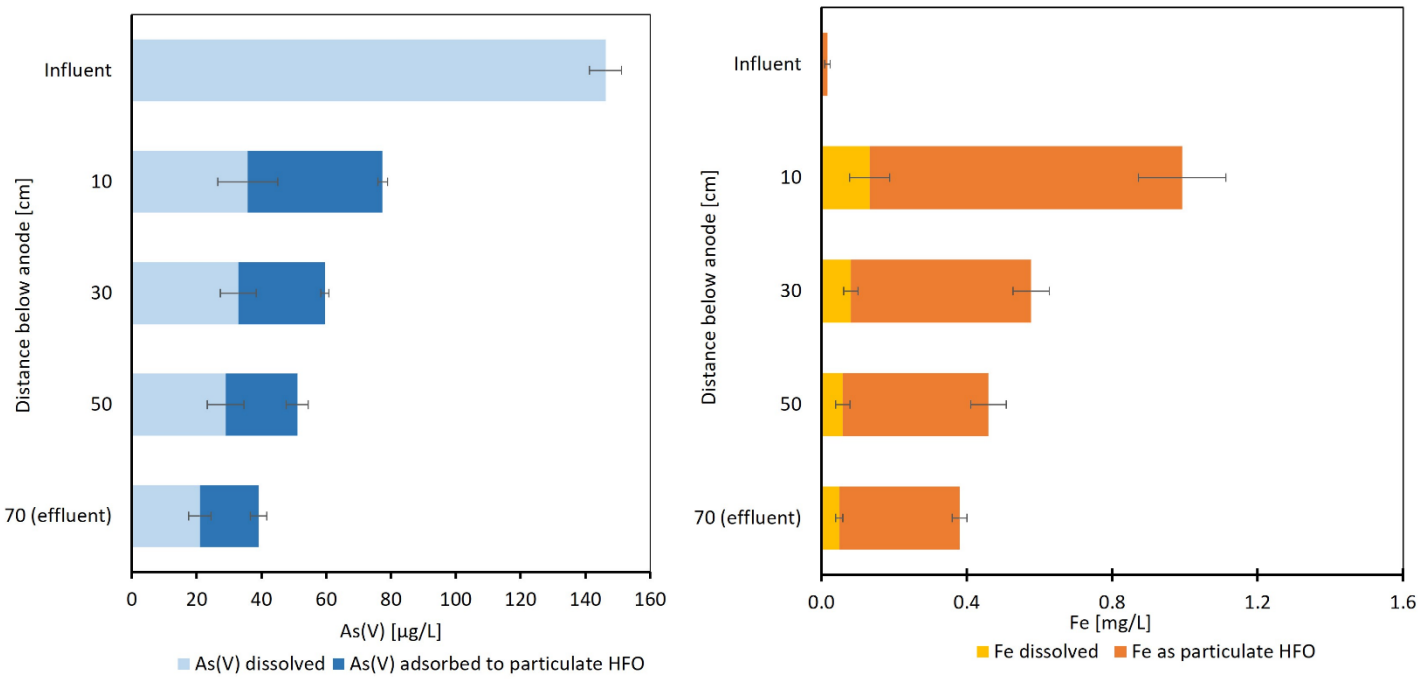

Fig. 12: Depth profile of As(V) (left) and Fe (right) at the 7th hour of operation for the As(V) reference flowthrough experiment (CD of 6.4 C/L, flowrate of 3 m/h and pH of 8). The As(V) graph presents dissolved As(V) and As(V) that has been adsorbed on iron flocks that have not been removed by the filter. The Fe graph gives the dissolved Fe concentrations and the concentrations of iron that was considered to be particulate HFO.

By operating the system at a CD of 9.4 C/L (2.7 mg/L theoretically dosed iron), the total arsenic concentration was reduced from 150 µg/L As(V) at the influent to 33 µg/L As(V) at the effluent. Of this 33 µg/L As(V), 22 µg/L As(V) was adsorbed to particulate HFO flocks (not yet removed by the filter material) and 11 µg/L was present as dissolved As(V). Considering the dissolved As(V), an As(V) removal efficiency of 93% and an Fe:As ratio of 19.4 was found. At 10 cm below the anode 1.17 mg/L of the released iron was present, indicating that already 57% had been removed. After the 70 cm of filter bed 2.26 mg/L of iron (84%) was retained and 2.67 mg/L (99%) had been oxidized. This iron retention resulted in a rise in supernatant of 2.3 cm after 7 hours of operation.

3.3.2 Increasing flowrate from 3 to 5 m/h

Operating the system at a high flowrate of 5 m/h with a CD of 6.4 C/L required a higher operational current of 0.040 A (40 mA), compared to the 0.023 A at 3 m/h. The arsenic and iron depth profiles taken at the 7th hour of operation (when the columns reached equilibrium) can be found in Fig. 13. In the effluent the dissolved As(V) was 29 µg/L, indicating that 81% of the 150 µg/L influent As(V) had been removed. A theoretical iron dosage of 1.85 mg/L for a CD of 6.4 C/L results in an Fe:As ratio of 15.3 [mg/mg]. From this 1.85 mg/L released iron, 1.7 mg/L (92%) was oxidized at 10 cm below the anode. In the 10 cm of anthracite below the anode, 23% of the total released iron (0.43 mg/L) was removed by the filter. 1.83 mg/L (94%) of the iron was oxidized and 1.43 mg/L (77%) of the iron was removed after 60 cm of additional filtration (with a residence time of approx. 7 minutes). At the end of the operational cycle of 7 hours, the supernatant level was 1.2 cm higher than at the beginning.

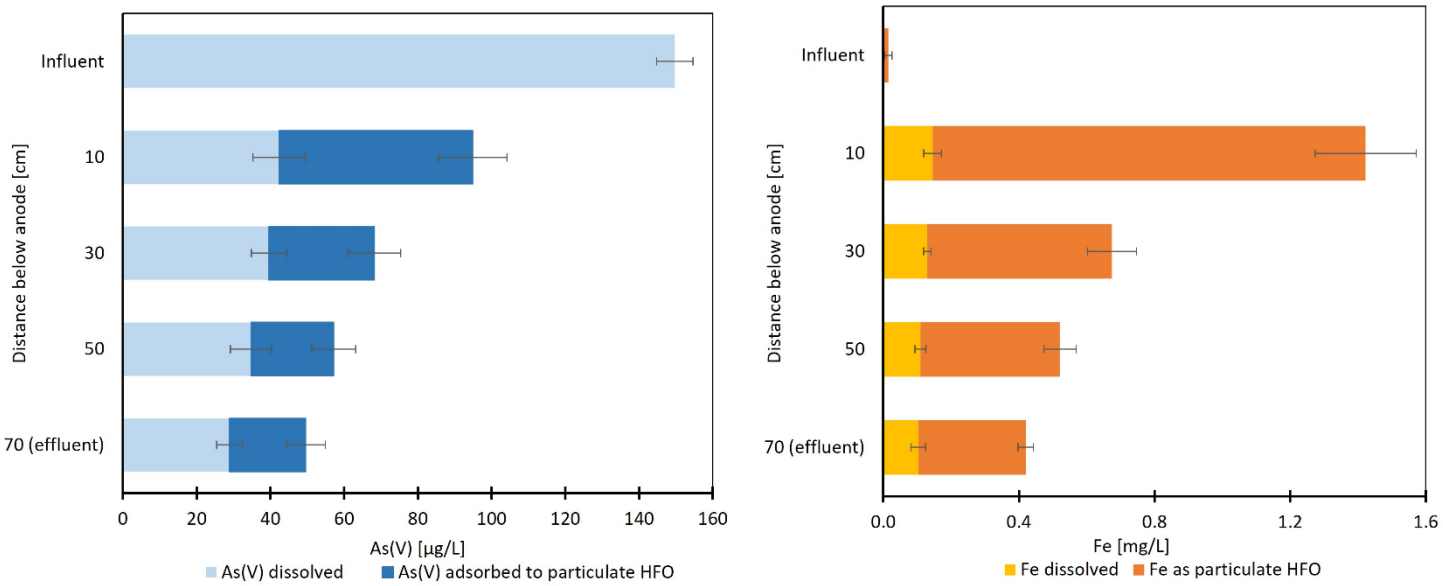

Fig. 13: Depth profile of As(V) (left) and Fe (right) for the As(V) flowthrough experiment with increased flowrate to 5 m/h at the 7th hour of operation. The As(V) graph presents dissolved As(V) and As(V) that has been adsorbed on iron flocks that have not been removed by the filter. The Fe graph gives the dissolved Fe concentrations and the concentrations of iron that was considered to be particulate HFO.

3.3.3 Lowering the pH from 8.0 to 7.0

As the pH of the tap water was relatively high (around 8.0), it was chosen to execute one set of experiments with the pH lowered to 7.0. The depth profile of the experiments executed with a pH of 7.0, operated at 3 m/h and a CD of 6.4 C/L, showed effluent concentrations of dissolved arsenic and arsenic adsorbed to iron precipitates of 7 and 10 µg/L respectively (Fig. 14). Regarding dissolved arsenic, a removal efficiency of 96% was found with an Fe:As ratio of 11.8 [mg/mg] for an influent arsenic concentration of 164 (+/- 7) µg/L. At 10 cm below the anode, just 0.54 (29%) and 0.22 mg/L (12%) of the released iron was oxidized and removed respectively. In the column effluent, 1.78 mg/L (96%) of the released iron was oxidized and 1.65 mg/L (90 %) was removed by the 70 cm of filtration. Observations showed a rise in supernatant of (+) 0.6 cm at the end of the 7 hours of operation.

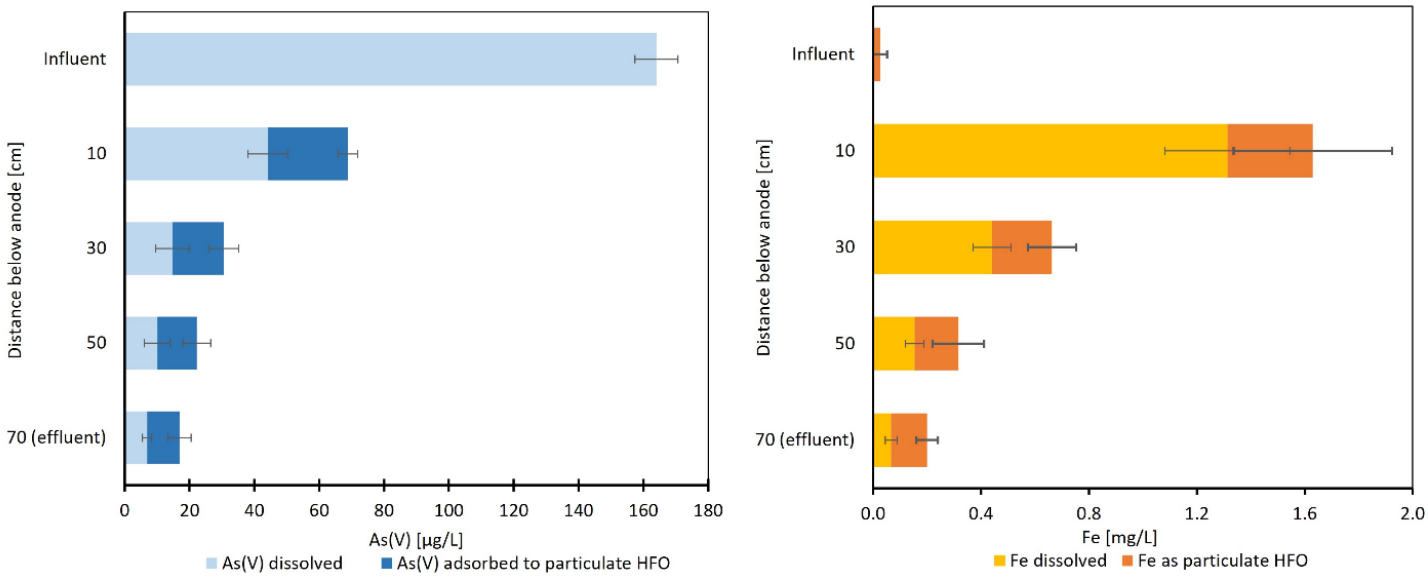

Fig. 14: Depth profile of As(V) (left) and Fe (right) for the As(V) flowthrough experiment with pH lowered to 7.0 at the 7th hour of operation. The As(V) graph presents dissolved As(V) and As(V) that has been adsorbed on iron flocks that have not been removed by the filter. The Fe graph gives the dissolved Fe concentrations and the concentrations of iron that was considered to be particulate HFO.

3.4 Biological As(III) oxidation

The columns with fresh anthracite were preloaded with tap water spiked with 150 (+/- 20) µg/L As(III) for over 9 weeks to establish an As(III)-oxidizing microbial community. During this preloading period, influent and effluent samples were analysed for dissolved As(V) and As(III) (Fig. 15). Limited arsenic oxidation was observed in the initial weeks, as the effluent arsenic was majorly As(III). After 6 weeks of operation, As(III) oxidation became clearly noticeable when approx. 50% of the influent As(III) was oxidized to As(V) in the effluent. This pattern of As(III) oxidation in the filter bed over time matches the findings from other studies focussing on establishment and characterisation of AsOB in sand filters (Gude et al., 2018b, 2018c; Roy et al., 2021).

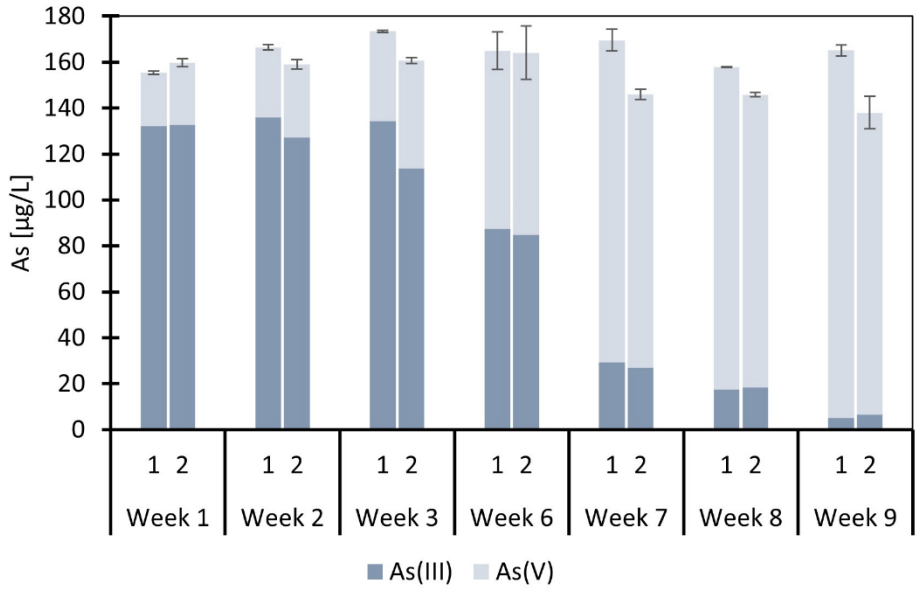

Fig. 15: As(III) and As(V) of the effluent of the duplicate AsOB columns, fed with tap water spiked with 150 (+/- 20) µg/L As(III).

In the 9th week of operation over 95% of the influent As(III) was oxidized to As(V) in the effluent of the two columns. The depth profile of the column was taken prior and after backwashing at the end of the 9th week to gain insights in the arsenic oxidation profile over depth and the effect of backwashing (Fig. 16). The As(III) oxidizing profile prior to backwashing is in line with the findings in a study of Yang et al. (2014), where after 20, 40, 60 and 80 cm of filter bed depth 50, 65, 80 and 90% of the influent As(III) (130 µg/L) was oxidized respectively (52, 74, 87 and 95% respectively for an influent arsenic concentration of 150 µg/L in this study). Despite focussing on an influent As(III) concentration of 10 µg/L in a study of Gude et al. (2018a) a similar trend was found, as over half of the influent As(III) was oxidized in the first 20 cm.

Due to backwashing of the filter, the arsenic oxidation in the first 20 cm decreased from 52 to 36% (Fig. 16). After 40, 60 and 80 cm of filter bed, 62, 76 and 91% of the influent As(III) was oxidized respectively after backwashing. In the top of the filter bed (after 20 cm) the difference in oxidation between prior and after backwashing is 14%. The deeper in the filter bed, so after 40, 60 and 80 cm, this difference decreases to 10, 9 and 4% respectively. This shows that deeper in the filter bed the effect of backwashing is less pronounced.

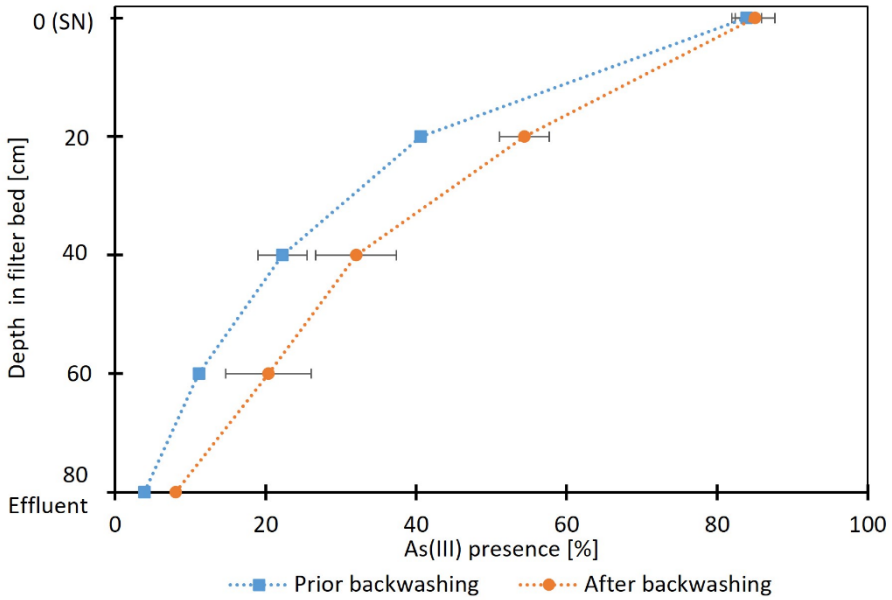

Fig. 16: Percentage As(III) of total arsenic over the depth profile of the fully ripened AsOB columns, prior and after backwashing. Error bars represent the deviation between the two sampled columns.

3.5 As(III) removal by electrodes embedded in the filter bed and in the supernatant

For the system with the electrodes embedded within the filter bed below a 50 cm thick arsenic oxidizing layer, 38 µg/L of total arsenic was found in the effluent at the 11th hour of operation. This 38 µg/L consisted of 29 µg/L dissolved arsenic (26 and 3 µg/L dissolved As(V) and As(III) respectively) and 9 µg/L of arsenic adsorbed to iron precipitates (Fig. 17). Based on the theoretical iron release of 1.85 mg/L for a CD of 6.4 C/L the dissolved arsenic removal resulted in an Fe:As ratio of 15.0. At 10 cm above the electrodes (after 40 cm of filter bed) 85% of the influent As(III) was oxidized, indicating proper functioning of the biological layer. Total arsenic concentrations (As(III) + As(V)) were constant in this first 40 cm. The release of iron in the filter bed by the electrodes can be observed based on the increase of iron concentrations from 0.03 to 0.6 mg/L after 40 and 80 cm of filter bed respectively. However, the iron concentration at 80 cm in the filter bed does not represent the amount of iron released by the Fe-EC system, as in the 30 cm below the electrodes iron is already oxidized and partly removed.

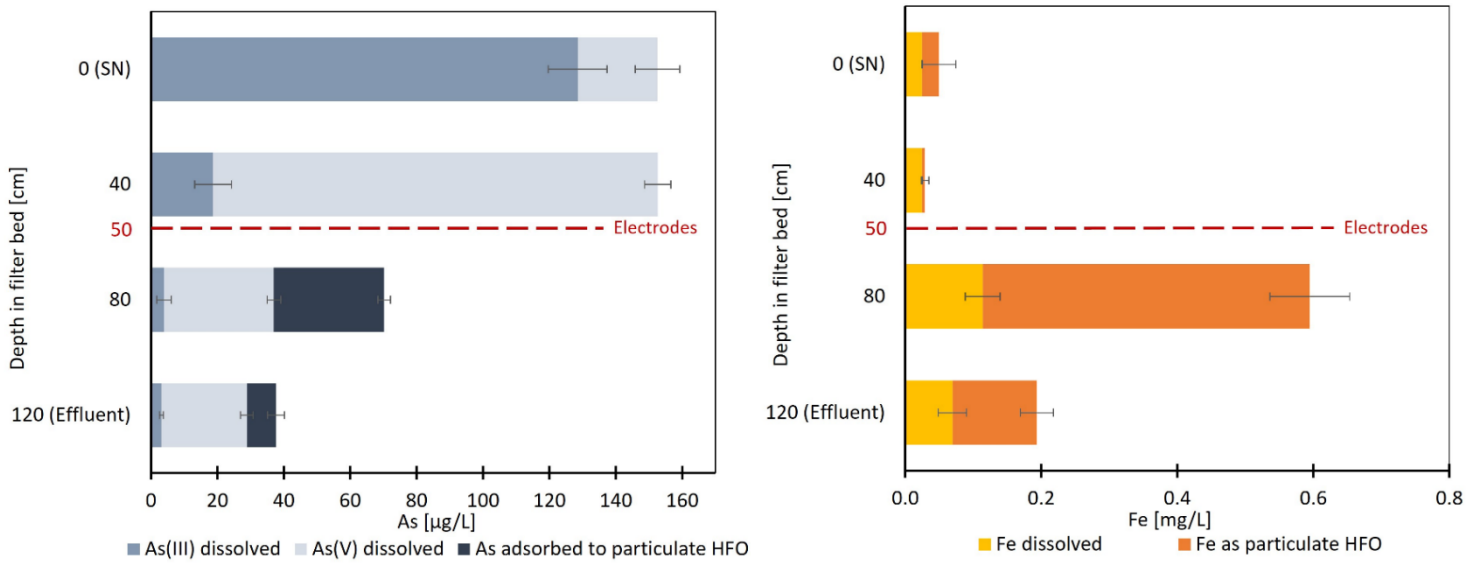

Fig. 17: Depth profile of As (left) and Fe (right) for the fully integrated electrodes in the flowthrough experiment using As(III). With a CD of 6.4 C/L (1.85 mg/L Fe), a flowrate of 3 m/h and a pH of 8.0.

The system with the electrodes in the supernatant showed 52 µg/L total arsenic in the effluent of the column at the 11th hour of operation (column in equilibrium). Of this 52 µg/L total arsenic, 49 µg/L was dissolved arsenic (47 and 2 µg/L dissolved As(V) and As(III) respectively) and 3 µg/L of arsenic adsorbed to iron precipitates (Fig. 18). This dissolved arsenic reduction implies that an Fe:As ratio of 18.3 is representative for operation with the electrodes in the supernatant. Iron concentrations in the supernatant were measured at 1.73 mg/L, while after 40 cm in the filter bed (at +80 cm) only 0.53 mg/L was found. In the effluent, 0.11 mg/L of total iron was still present.

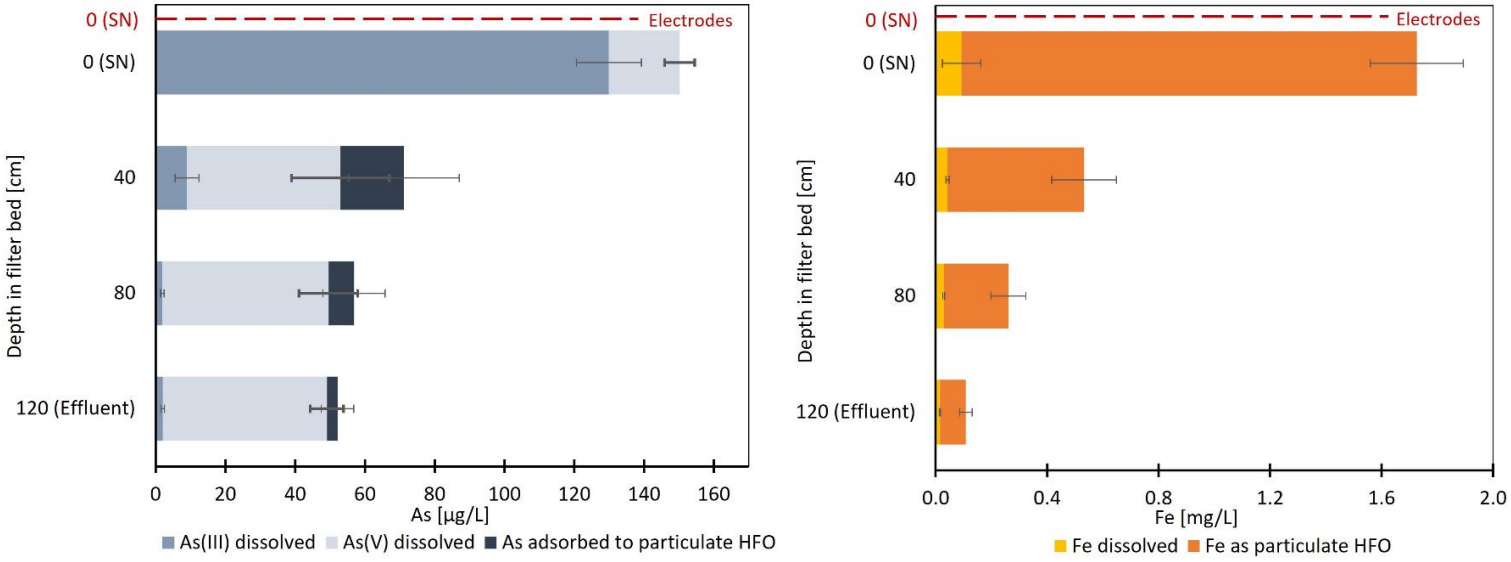

Fig. 18: Depth profile of As (left) and Fe (right) for the electrodes placed in supernatant water in the flowthrough experiment using As(III), sampled at the 11th hour of operation. With a CD of 6.4 C/L (1.85 mg/L Fe), a flowrate of 3 m/h and a pH of 8.0.

3.6 Energy consumption

During all Fe-EC flowthrough experiments the fate of energy consumption over the duration of the experiments was monitored. As the hourly water production varied for different flowrates, the energy consumption over time was converted to the energy consumption per volume of water treated (kWh/m^3) (Fig. 19). For a charge dosage of 6.4 C/L in the reference and pH 7.0 experiments with the electrodes in the filter bed, the initial energy consumption was of the same order at 0.014 and 0.012 kWh/m^3 respectively. However, while operating the electrodes in the filter bed at 5 m/h and CD of 6.4 C/L, a higher initial energy consumption of 0.022 kWh/m^3 was observed. Further, for a CD of 9.4 C/L the initial energy consumption was the highest of all operating conditions at 0.030 kWh/m^3. For all experiments with the electrodes in the filter bed it was observed that there was an increasing pattern in the energy consumption. This increasing trend seemed to be dependent on the operating conditions, which was most pronounced for the experiments using a CD of 9.4 C/L. With the electrodes in the supernatant, operated at a CD of 6.4 C/L, the initial energy consumption was just at 0.007 kWh/m^3. For the electrodes in the supernatant there was no distinct increasing or decreasing pattern visible in the energy consumption visible as more water was treated.

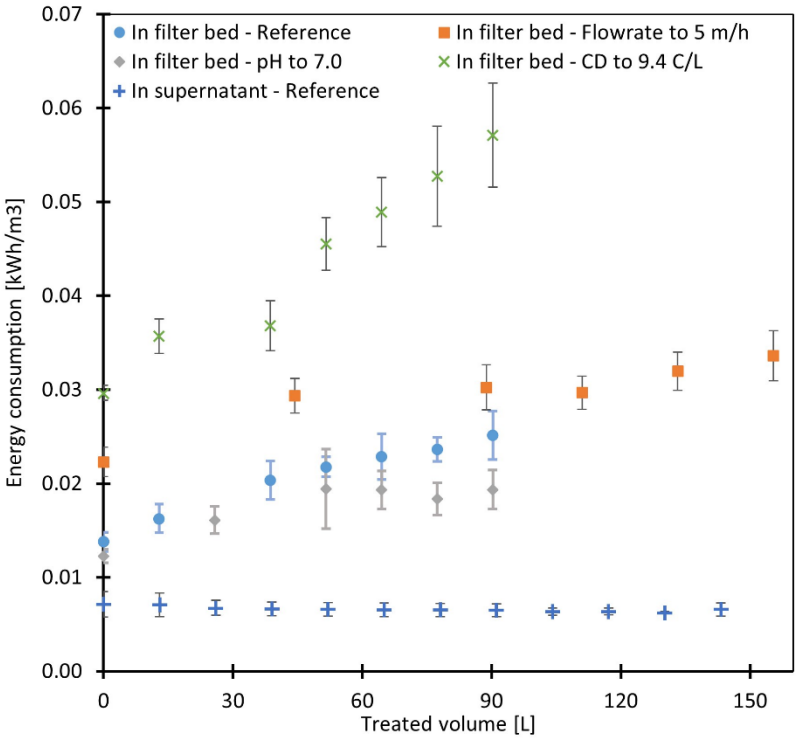

Fig. 19: Energy consumption over duration of experiment for different operational conditions. With the reference operated at a CD of 6.4 C/L, a flowrate of 3 m/h and a pH of 8.0.

4. Discussion

4.1 Non-uniform iron distribution for integrated electrodes

Iron release experiments in paragraph 3.2 showed that the iron release by the anode in the filter bed resulted in a non-uniform iron distribution ranging between 1 and 4 mg/L (1.85 mg/L avg.). As the cathode, placed above the anode, had a smaller dimension than the anode (diameter of 55 and 75 mm respectively) it might have influenced the homogeneity of the iron release. Corrosion of the crocodile clamps, connecting the wires from the DC source to the anode, was clearly observed when comparing the clamps prior and after the experiments. The crocodile clamps (made of mild steel) apparently released iron and thereby influenced the uniformity of the iron release pattern. However, no clear pattern could be found showing that the release of iron was depended on how the electrodes were connected to the DC power source.

It was hypothesised that the non-uniform iron distribution in the filter bed affected the arsenic removal efficiency. As(V) removal experiments were executed and compared to the results of batch experiments to investigate the consequences of non-uniform iron concentrations on the arsenic removal performance (Table 5). With a CD of 7.1 and 8.4 C/L dissolved As(V) concentrations were reduced to 8.5 and 7.7 µg/L respectively in the batch experiments. However, dissolved As(V) concentrations in the flowthrough system were only reduced to 21 and 11 µg/L for a CD of 6.4 and 9.4 C/L respectively. When considering Fe:As ratio for a CD of 6.4 C/L a value of 13.2 was expected based on the batch experiments, however a value of 14.3 was found in the flowthrough system. The same pattern was found for a CD of 9.4 C/L, as the expected Fe:As ratio from the batch experiments (18.7) was lower than found in the flowthrough results (19.4).The arsenic removal values and Fe:As ratios both indicate a reduced arsenic removal efficiency when integrating the electrodes in the filter bed.

Table 5: Comparison of As(V) removal efficiency and Fe:As ratios between batch and flowthrough experiments.

CD [C/L]	Removal efficiency [%]		Fe:As ratio	
	Batch	Flowthrough	Batch	Flowthrough
6.4	93	86	13.2	14.3
9.4	97	93	13.2	19.4

In the flowthrough As(V) experiments, a large amount of the released iron was already oxidized and removed in the first 10 to 30 cm below the anode (50 to 70% iron removal), which is in line with previous findings showing rapid removal of iron in RSF (Gude, et al., 2018b; Yang et al., 2014). The drawback of this rapid iron oxidation and removal is the limited mixing of the iron with the bulk solution, as it was shown that approx. 60 to 70 cm was needed to achieve an uniform iron concentration by mixing in the filter bed (paragraph 3.2). The combination of a partly homogeneous iron release by the anode and limited mixing in the filter bed caused a non-uniform iron distribution. These observations of reduced arsenic removal performance by improper mixing are in line with other studies where iron was chemically introduced in the filter bed (Gude et al., 2018a; Sharma et al., 2001). A lack of iron (or lower concentrations) in certain areas affected the arsenic removal efficiency, caused

by the short-circuiting of the water past the iron. Other studies confirm the importance of mixing of the released iron with the bulk solution to enhance arsenic removal (Goren et al., 2020; Li et al., 2012; Martínez-Villafañe et al., 2009).

4.2 Effect of CD, flowrate and pH on operational performance

4.2.1 Operating conditions affecting As(V) removal

When increasing the CD from 6.4 to 9.4 C/L, dissolved As(V) concentrations were reduced from 21 to 11 µg/L in the effluent and the removal efficiency rose from 86 to 93% accordingly (removal of approx. 129 and 139 µg/L dissolved As(V) respectively). One-way Anova analysis showed significant differences ($p < 0.05$) in effluent dissolved arsenic concentrations when comparing the results of the two CD conditions. An increase in total iron concentration from 0.99 to 1.17 mg/L at 10 cm below the anode confirmed that indeed more iron was released by the electrodes for a higher CD. Both observations are in line with the batch experiments, where the As(V) removal and iron production increased with a higher CD (Fig. 9).

An increase in flowrate from 3 to 5 m/h (for a similar CD of 6.4 C/L) resulted in an increase of effluent dissolved As(V) from 21 to 29 µg/L and a corresponding increase in Fe-As ratio from 14.3 to 15.3. The dissolved arsenic concentrations in the effluent when increasing the flowrate from 3 to 5 m/h showed significant differences according the one-way Anova analysis ($p = 0.03$). Compared to the 3 m/h (reference) As(V) depth profile, the 5 m/h profile showed elevated levels of dissolved As(V) over the entire depth profile below the electrodes (Fig. 20). These results are contrary to the hypothesis that arsenic removal would be higher for a higher flowrate, as it was expected that an increase in turbulence and iron penetration would result in better mixing. Iron flocks indeed penetrated deeper into the anthracite bed when increasing the flowrate (Fig. 20), which was also found in other studies (Gude, et al., 2018b). Especially in the first 10 to 30 cm where the iron concentrations rose from 1 to 1.4 mg/L and 0.58 to 0.68 mg/L respectively. However, it is expected that an increase in short-circuiting of As(V), past the generated iron flocks, with increasing flowrates caused the decrease in removal of dissolved arsenic. With the higher flowrates the residence time reduced and there was less time for proper mixing of the arsenic with the released Fe. Additionally, the increase of dissolved iron concentration in the effluent (from 0.05 to 0.11 mg/L) when increasing the flowrate had an adverse effect on the removal of dissolved arsenic. With the reduced iron oxidation due to a reduced residence time in the filter bed (from 12 to 7 minutes), there was less iron available for arsenic adsorption resulting in lower removal of dissolved arsenic.

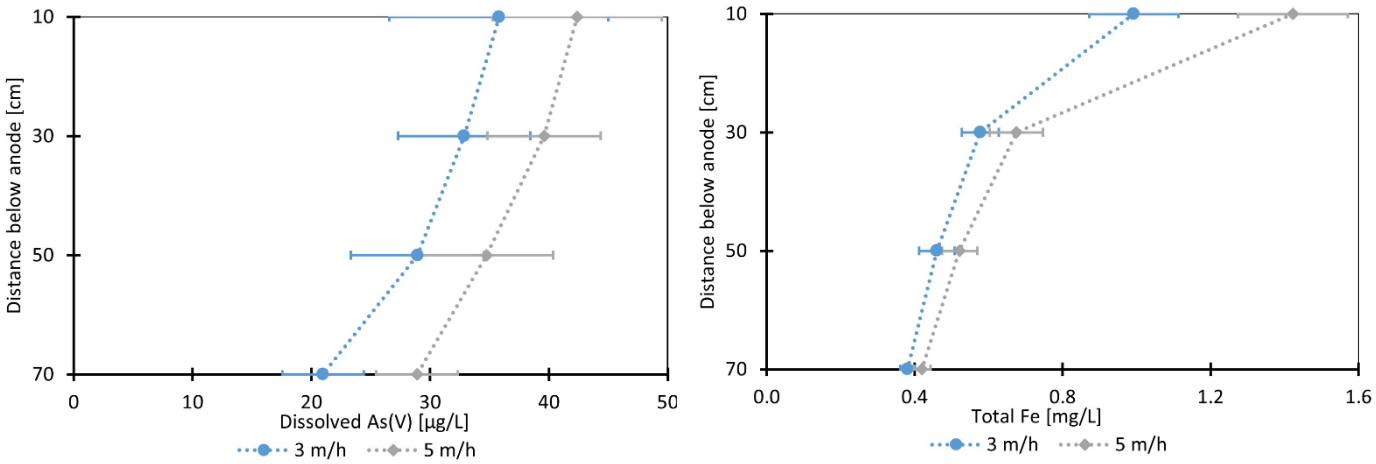

Fig. 20: Comparison of depth profiles for flowrates of 3 and 5 m/h, with dissolved As(V) (left) and total iron (right).

Reduction of pH from 8.0 to 7.0 improved the systems arsenic removal performance as the dissolved As(V) in the effluent reduced from 21 to 7 µg/L (significantly different results according Anova analysis, as $p < 0.05$). This increase in arsenic removal resulted in a decrease in the Fe:As ratio from 14.3 to 11.8 [mg/mg]. These findings are in line with the results of batch experiments in other studies where it was concluded that lowering the pH from 8/9 to neutral pH (pH 7.0) improved As(V) adsorption to Fe(III) (oxyhydr)oxides (Dixit & Hering, 2003; Delaire et al., 2017; van Genuchten et al., 2020). Additional to the improved adsorption of As(V) to iron precipitates at pH 7.0, it was hypothesised that mixing of the iron with the As(V) in the filter bed was improved when slowing down the iron oxidation by lowering the pH (Katsoyiannis et al., 2008a). Enhanced mixing would reduce the effect of short-circuiting and improve the systems arsenic removing performance. At 10 and 30 cm below the anode, 1.3 and 0.45 mg/L of dissolved iron was respectively present in the pH 7.0 experiments (Fig. 21). For the experiments executed at pH 8.0 only 0.13 and 0.08 mg/L of dissolved iron was present at 10 and 30 cm below the electrode respectively (Fig. 21). The elevated levels of dissolved iron in the layers below the electrodes in the pH 7.0 experiments promoted iron mixing and improved the arsenic removal. Reduced loss of iron on top of the anode can be another reason for the improved dissolved As(V) removal. As with low pH the iron oxidation is slower, the iron is more likely to be transported away from the area at the top of the anode and less iron is ‘lost’ in the no-flow zones.

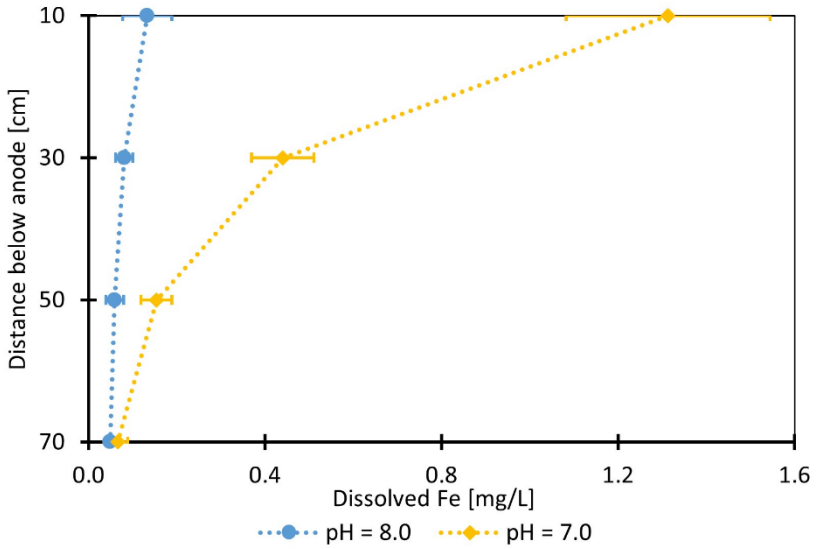

Fig. 21: Comparison of depth profiles of dissolved iron for a pH of 8.0 and 7.0.

4.2.2 Operating conditions affecting supernatant rise

Another way to assess the performance of the different operating parameters is in terms of supernatant (SN) rise. As iron is captured in the filter bed of the RSF the bed clogs and the resistance of the filter bed increases. This increase in resistance requires an increase in supernatant level to keep operating the RSF at a constant flowrate. The higher the supernatant rise over the operational period, or per volume of water treated, the more frequent the filter has to be backwashed. From an operational and cost perspective it is desired that the backwashing frequency is as low as possible.

The rise of SN level was monitored during all experiments and was evaluated per 100 L of water treated (Table 6). Additionally, the amount of iron that was retained per 100 L water treated was estimated based on the effluent iron concentrations. The SN rise was largest for the operation at increased charge dosage (to 9.4 C/L), as more iron was generated and captured (228 vs. 147 mg) caused the bed to clog faster than during the reference experiment. Slightly less iron was captured in the filter bed of the 5 m/h experiment as 3% less iron was captured (4 mg) after treating 100L of water, additionally the rise of supernatant level was 54% lower (0.9 cm). The experiments with the pH lowered to 7.0 showed better iron removal compared to the reference experiment as 12% more iron was removed (18 mg). This increased removal could be explained by the formation of larger flocks caused by the point of zero charge for iron molecules at pH 7.0 (Hove et al., 2008; Schwertmann & Cornell, 2000). Despite the increased iron retention the rise in SN level was 60% (1 cm) lower. Deeper penetration of iron in the high flowrate and low pH experiments minimized localized clogging of the filter bed just below the anode, resulting in lower head losses and SN rise (Fig. 20 and 21).

Table 6: Supernatant water level rise during operation for different operating conditions. The rise in supernatant was calculated based on 7 hours of operation and evaluated per 100 L of water treated. The reference system was operated at 6.4 C/L, a flowrate of 3 m/h and pH of 8.0.

	Reference	**CD to 9.4 C/L**	**Flowrate to 5 m/h**	**pH to 7.0**
Rise supernatant level per 100 L [cm]	+ 1.7	+ 2.5	+ 0.8	+ 0.7
Iron retained per 100 L [mg]	147	228	143	165

4.2.3 Operating conditions affecting energy consumption

As the release of iron is controlled by operating the Fe-EC system at a certain electrical current, the energy consumption of the system is a relevant operational parameter to consider. Energy consumption is evaluated as the energy needed to treat 1 m^3 of water, expressed in kWh/m^3 (eq. 7.). As the energy consumption is dependent on the applied electrical current, it can be related to the iron release by Faraday's law (eq. 5) and the arsenic removal efficiency.

$$\text{Energy consumption [kWh/m}^3\text{]} = U\,[V] * I\,[A] / Q\,[m^3/h] \quad (7)$$

When increasing the flowrate from 3 to 5 m/h (for similar CD) the initial energy consumption rose from 0.014 to 0.022 kWh/m^3 (Fig. 22). This difference was caused by the increasing voltage during operation and can be related to the linear relation between current, voltage and resistance (Ohm's law) in the electrochemical cell. For an increasing flowrate (and similar CD) the amount of current dosed per m^3 (I / Q) was constant at 1.75 A/m^3. This implies that the voltage had to be constant for the energy consumption to be stable (eq. 7). To ensure a CD of 6.4 C/L when increasing the flowrate from 3 to 5 m/h, a higher operational current was applied as more iron was released per unit of time (0.023 to 0.040 A). This increase in operational current required higher voltages to operate the electrochemical cell (8 to 12.5 V), which caused the increase in energy consumption when increasing the flowrate (eq. 7). This theory implies that operating the system at lower iron dosages did not only influence the energy consumption by a lower I / Q – ratio, but additionally by the reduced voltages during operation (eq. 7). This effect was clearly visible when the CD was increased from 6.4 to 9.4 C/L (increase in iron dosage of 47%), as the initial energy consumption rose from 0.014 to 0.03 kWh/m^3 (increase of 114%).

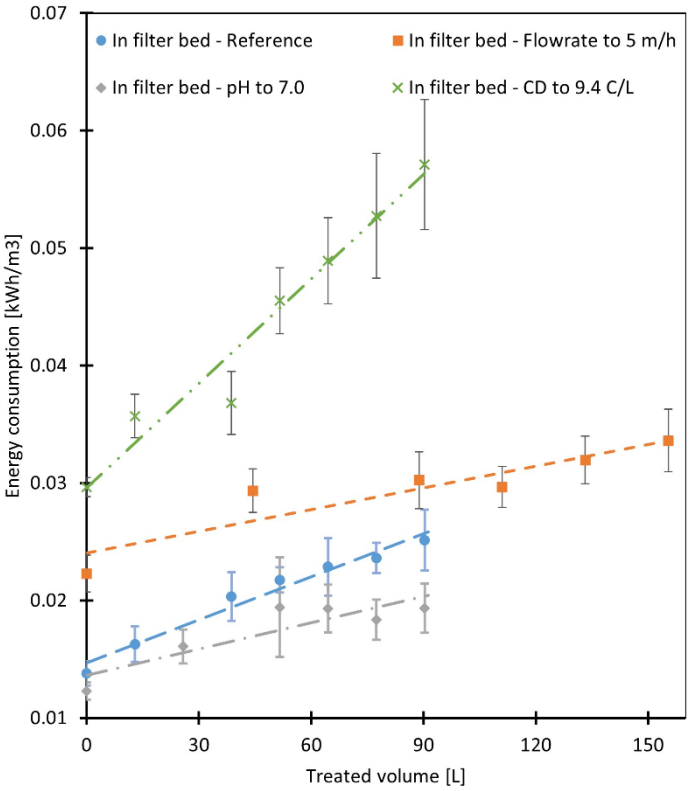

Fig. 22: Fate of energy consumption for the electrodes in the filter bed with linear estimations. With the reference operated at a CD of 6.4 C/L, a flowrate of 3 m/h and a pH of 8.0.

The voltage required to operate the electrodes in the filter bed increased during the system's operation, resulting in an increased energy consumption during treatment (Fig. 22). This increase in voltage indicates an increase in resistance of the electrochemical cell, as the dosed current per m^3 (I/Q – ratio) was constant. Other studies also observed this increase in cell resistance over time, related to the formation of surface layers at the anode and cathode (Amrose et al., 2014; Kobya et al., 2011; Müller et al., 2019). However, in those studies only a minor rise in voltage was observed over extended operational timeframes. This difference could be explained by the location of the electrode, as the electrodes in the previously mentioned studies were vertically placed in a bulk solution. With the electrodes horizontally placed in the anthracite (for a homogeneous iron release), dead zones occurred on the upstream (top side) of the anode and the iron was not transported away effectively. It has been shown that low turbulence with limited transport of iron away from the electrodes promotes the formation of the passivation layers (Flores et al., 2013; Mollah et al., 2004). It is hypothesised that this relative rapid increase in resistance was caused due to entrapment of the generated iron precipitates between the anode and cathode. Iron precipitates that were captured by the anthracite in between the anode and cathode increased the resistance of the cell and so the operating voltage and energy consumption (Chen et al., 2014). This hypothesis suggest a linear behaviour in the increase in resistance, as during normal operation iron is released at the same rate over time and is expected to accumulate between the electrodes. The observed increasing energy consumption indeed showed this expected linear behaviour (Fig. 22), which suggests that the behaviour could be explained by the aforementioned hypothesis. Analysis of the anode surface at the end of operation could confirm this

hypothesis of surface/passivation layer formation, as a brownish rust layer is clearly visible at the surface of the anode at the top of the horizontally placed electrode (Fig. 23).

Fig. 23: Anode condition after 7 hours of operation for integrated electrodes in the reference experiments. Top of the horizontally placed anode (left) and bottom (right) with clear differences in surface layer formation

The aforementioned mechanisms could explain a higher rise in energy consumption when the iron dosage increased from 6.4 to 9.4 C/L (+0.013 vs. +0.029 kWh/m^3 after treating 100 L of water), visible as a steeper slope compared to the reference conditions (Fig. 22). As more iron was generated, more precipitates were formed and captured between the anode and cathode, which increased the resistance and so the required voltage of the cell during operation. The observed reduced energy consumption when lowering the pH from 8.0 to 7.0 (+0.011 to +0.007 kWh/m^3 after treating 100 L of water) and the shallower increasing slope per volume of water produced is in line with the hypothesis. The slower iron oxidation at lower pH resulted in the transport of iron away from the electrodes (as was observed in paragraph 3.3, Fig. 12 and 14) and reduced the precipitate formation on top of the anode. In the higher flowrate experiments, the increase in energy consumption per 100 L of treated water was the lowest at +0.008 kWh/m^3. With a higher flowrate the increase in turbulence of the water near the anode promoted the transport of iron away from the anode which was observed in section 4.2.1 (Fig. 20) and is confirmed by literature (Flores et al., 2013; Mollah et al., 2004). This reduced the formation of passivation layers and the amount of precipitates captured between the electrodes, which minimized the increase in cell resistance. One-way Anova analysis showed that the increase in energy consumption during all of the aforementioned experiments (with a changed operational parameter) differed significantly from the reference experiment ($p < 0.05$).

4.3 Performance evaluation of biological arsenic oxidation

4.3.1 Reliability during continuous operation and backwashing

For design purposes of the fully integrated system with the electrodes embedded in the filter bed, it was desired that during daily operation and backwashing a large fraction of the As(III) was oxidized before the water passed the electrodes. In earlier studies, the (short term) effect of backwashing on the As(III) oxidation over depth in RSF was not investigated. As mentioned, remarkable

changes in stratified removal pattern were observed after backwashing the AsOB growth column, as after the first 20 cm the As(III) oxidation decreased with 14%. Deeper in the filter bed (after 60 cm additional filtration) the difference in As(III) oxidation was reduced to only 4%. The first backwash after 9 weeks caused the first 20 cm with high biological activity to be mixed with the rest of the filter bed. This resulted in lower biological activity and reduced As(III) oxidation in the top of the filter and more arsenic oxidation in the middle and bottom of the filter, causing the increase of oxidation in deeper layers of the filter bed. The observed differences between prior and after backwashing were likely caused by the fact that the bed had not been backwashed for 9 weeks. Results of the fully integrated system with the electrodes deeper in the filter bed (without effect of the Fe-EC system) show that after 40 cm the As(III) oxidation was consistent, as over multiple days of operation 85 (+/- 5) % of the influent As(III) was oxidized. Daily backwashing and additional ripening of the biomass resulted in neglectable differences in the stratified arsenic oxidation profile over depth, caused by frequently re-ordering the top layer with highest biological activity. Therefore it can be concluded that daily backwashing did not affect the arsenic removal efficiency of the system. These findings match the results from experiments with ammonium oxidizing bacteria in RSF, where backwashing did not affect the stratified removal profile of ammonium over depth (Lee et al., 2014).

4.3.2 Fe-EC with subsequent biological arsenic oxidation enhancing arsenic removal

Dissolved arsenic concentrations were reduced from 150 to 49 µg/L (Fe:As of 18.3) with the electrodes operated at 6.4 C/L located in the supernatant water of a RSF with biological arsenic oxidation. In As(III) Fe-EC batch experiments with similar water characteristics in the study of Roy et al. (2021), it was observed that for a reduction from 150 to 50 µg/L of dissolved arsenic a CD of approx. 22 C/L (6.4 mg/L Fe) was needed (Fe:As of 64). Apparently, arsenic removal can be enhanced by operating Fe-EC in the supernatant of a RSF with biological arsenic oxidation in a flowthrough system. This enhanced removal can be explained by the penetration of iron precipitates into the filter bed, in which As(III) was oxidized to As(V) (Fig. 24). Because arsenic removal by iron can be enhanced when As(III) is oxidized to As(V) due to higher sorption affinities (Bissen & Frimmel, 2003; Dixit & Hering, 2003; Li et al., 2012), improved arsenic removal is achieved as an estimated 85% of the As(III) is biologically oxidized to As(V) in the presence of iron in the filter bed.

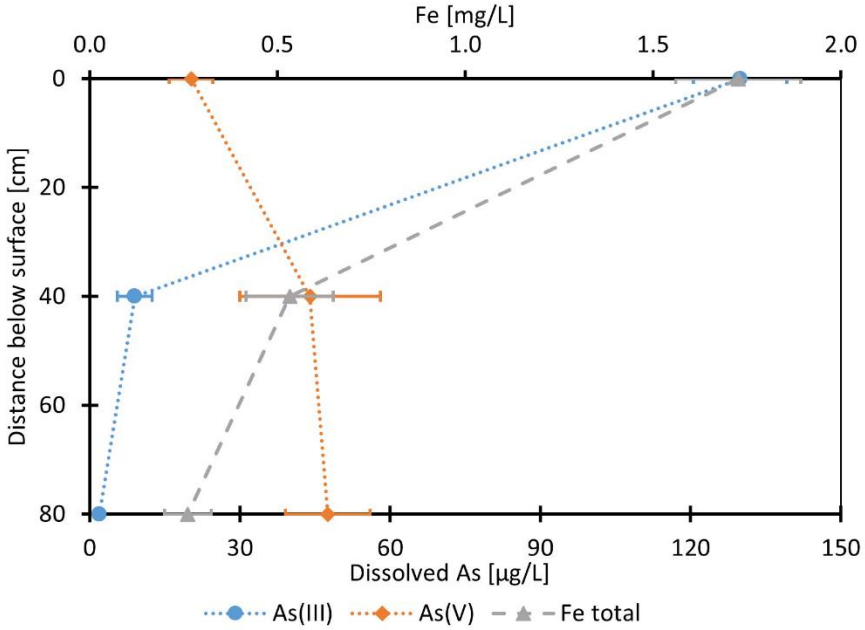

Fig. 24: Depth profile for As(III), As(V) and total Fe for the system with electrodes in the supernatant.

4.4 Effect of electrode location in a As(III) oxidizing and removing system

4.4.1 Electrode location affecting arsenic removal efficiency

With the objective to reduce the iron dosage when removing arsenic during groundwater treatment, the arsenic removal performance of the integrated electrodes was compared against the electrodes within the supernatant. It was hypothesised that the introduction of iron after biological As(III) oxidation (electrodes in the filter bed) instead of prior to this oxidation (electrodes in the supernatant) would enhance arsenic removal. Results indeed showed an improved arsenic removal, as dissolved arsenic concentrations in the effluent were reduced from 49 to 29 µg/L and the Fe:As ratio decreased from 18.3 to 15.0, when placing the electrodes in the filter bed (Fig. 25). One-way Anova analysis showed that the effluent concentrations for the two electrode locations were significantly different ($p < 0.05$). The aforementioned hypothesis was based on the 2-step arsenic removal mechanism for the electrodes in the filter bed, where the influent As(III) was first oxidized to As(V) and subsequently adsorbed to the iron introduced in the filter bed (Gude et al., 2018a; Roy et al., 2021). The depth profile of As(III) showed that after 40 cm of filtration through the biologically active filter bed (just above the electrodes) the 129 µg/L influent As(III) was reduced to 19 µg/L (110 µg/L oxidized) which resulted in an increase of As(V) from 24 to 134 µg/L (Fig. 25). After passing the iron generated at the electrodes, dissolved As(V) concentrations decreased from 134 to 33 µg/L after 30 cm of anthracite. This shows the principle of As(III) oxidation being the first step to ensure improved arsenic adsorption and removal when applying Fe-EC in the filter bed. Future XAS results will show what kind of iron solids were generated, but most importantly whether As(V) and/or As(III) was adsorbed. This will proof whether the initially assumed mechanisms improved the arsenic removal.

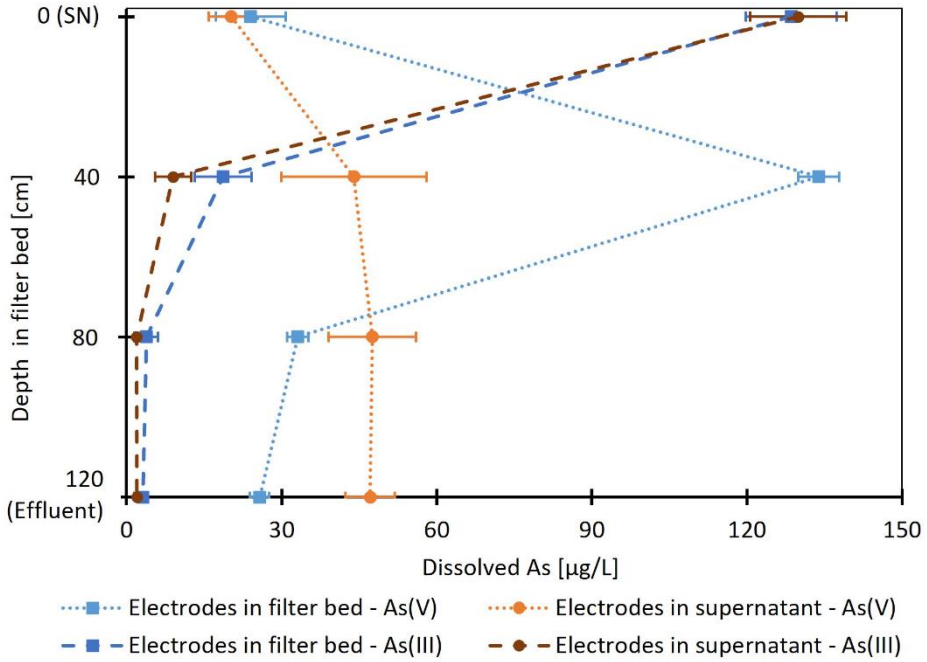

Fig. 25: Comparison of depth profiles for As(III) and As(V) between electrodes in the filter bed and supernatant.

Despite iron being present in deeper layers when the electrodes where placed in the supernatant (0.53 and 0.26 mg/L after 40 and 80 cm of filtration respectively), no additional dissolved As(V) was removed in the bottom 80 cm of the filter (Fig. 25). Similar behaviour was observed in another study, where it was observed that the present HFO flocks deeper in the filter bed did not absorb any additional As(V) (Gude et al., 2018a).

4.4.2 Impact of electrode location on energy consumption

Differences in the initial energy consumption and the behaviour over time were observed when comparing the two electrode locations (in filter bed vs. supernatant). 0.014 kWh/m^3 was observed as the initial energy consumption for the electrodes in the filter bed, while for the electrodes in the supernatant it was only half at 0.007 kWh/m^3. Even though both systems were operated at similar operating conditions (CD of 6.4 C/L at a current of approx. 0.023 A), these significant differences ($p < 0.05$) were observed. The operational voltage proved to be double when placing the electrodes in the filter bed (8.1 V), compared to the electrodes placed in the supernatant water (4.1 V). The anthracite present in between the anode and cathode (when placed in the filter bed) caused an increase in resistance of the electrochemical cell, which required higher voltages to operate the system. This increase in operational voltage inevitably resulted in an increase in energy consumption of the system (eq. 7).

Similar to the observations of an increasing energy consumption over time in the As(V) experiments (paragraph 3.6), the energy consumption increased for the electrodes in the filter bed in the fully integrated system (+0.003 kWh/m^3 after treating 100 L of water). Contrary to this rise is the constant energy consumption for the electrodes placed in the supernatant level. A new set of

electrodes was used at the start of the experiments to eliminate possible effects of electrode aging. With the electrodes in the supernatant, iron precipitates were transported away and did not accumulate in the anthracite present in between the electrodes. This prevented the increase of cell resistance and so the increase in energy consumption over time. Additionally it is hypothesised that the difference in the formation of surface layers caused differences in cell resistance over time. Contrary to the surface layer on the anode in the filter bed which could only be removed using sand paper and an acid wash, the surface layer on the anode in the supernatant looked fluffy and could easily be removed by a paper towel or a soft brush (Fig. 25). The observations of the short term formed surface layer on the anode seem to be in line with other studies where the electrodes had been placed in a water source (Müller et al., 2019). Based on the long term field study of Amrose et al. (2014) in West-Bengal, it is expected that operation of the electrodes in the supernatant for a longer timeframe will ultimately increase the voltage and so the energy consumption of the system.

Fig. 26: Comparison of anode condition after operation when placed in the supernatant (left) and in the filter bed (right).

4.4.3 Considerations for system improvement and re-design

It was shown that the performance of the electrodes in the filter bed could be enhanced by changing different operating conditions (paragraph 4.2). This performance can be evaluated in terms of arsenic removal efficiency, as it is desired that the iron released in the filter bed removes as much arsenic as possible. The lower the Fe:As ratio the more arsenic is removed with the same amount of iron, ultimately resulting in lower amounts of iron to be dosed. The rise in supernatant level (and so the backwashing frequency) and the energy consumption per m^3 of treated water are additional considerations when operating a system. Table 7 gives an evaluation of the performance parameters for the different operating conditions which can be used to improve overall system performance. This evaluation should just be used as an indication, as values will not be representable for (ground)water with other characteristics. Only measurable outcomes of this study have been presented, other factors as ease and cost of implementation have not been considered.

Table 7: Comparison of operational performance for different operating conditions as outcomes of As(V) removal experiments with integrated electrodes.

	Reference	CD to 9.4 C/L	Flowrate to 5 m/h	pH to 7.0
Effluent dissolved As [µg/L]	21	11	29	7
Fe:As ratio	14.3	19.4	15.3	11.8
SN rise [cm/100 L]	+ 1.7	+ 2.5	+ 0.8	+ 0.7
Energy consumption (initial) [kWh/m^3]	0.014	0.030	0.022	0.012
Energy consumption increase after 100 L [kWh/m^3]	+0.013	+0.029	+0.008	+0.009

Legend for table 7

	Description
	Best (1st) performing operational parameter in performance class
	2nd performing operational parameter in performance class
	3rd performing operational parameter in performance class
	Worst (4th) performing operational parameter in performance class

Lowering the pH to 7.0 seems to be an effective way to enhance the performance of the electrodes in the filter bed, as the arsenic removal is maximized for minimal iron dosage, based on the highest arsenic removal with the lowest Fe:As ratio. Furthermore the supernatant rise and rise in energy consumption were relatively low when the pH was reduced from 8.0 to 7.0. However, it will be undesirable to dose chemicals (acid) to lower the pH of the influent as chemicals require proper handling, storage, transport and high costs. A delayed/limited aeration step prior to the sand filter, as was applied in a study of Annaduzzaman et al. (2021), would enable to operate the system at lower pH without having to dose chemicals as raw groundwaters generally have low pH. Another way to enhance the performance of the electrodes in the filter bed is by increasing the thickness of the biologically active layer on top of the electrodes. During the fully integrated As(III) experiments some As(III) was still present near the electrodes in the filter bed (estimated between 5 and 15 µg/L). The presence of As(III) resulted in a higher arsenic effluent concentration (21 vs. 29) and Fe:As ratio (15.0 vs. 14.3) compared to the As(V) experiment under similar operating conditions. Because not all As(III) was oxidized to As(V) prior to passing the electrodes a fraction of the present arsenic could not be adsorbed effectively and the arsenic removal performance decreased (Dixit & Hering, 2003; Delaire et al., 2017; Hug & Leupin, 2003). By increasing the thickness of the biologically active layer more As(III) would be oxidized to As(V) prior to the electrodes, improving the overall arsenic removal. Additionally, the performance regarding the energy consumption of the proposed system can be improved by optimizing electrode characteristics resulting in a lower energy consumption. Restrictions in available space within the column caused the cathode to be designed smaller than the anode (55 vs. 75 mm diameter) so it was possible to connect the crocodile clamps to the electrodes from the DC power source. Increasing the cross sectional area of the electrodes, or by reducing the distance between

anode and cathode, would reduce the operating voltage of the cell and so the energy consumption of the system (Mollah et al., 2004). A potential drawback of reducing the inter electrode distance is the elevated pH near the anode which is a consequence of placing the cathode close to the anode, resulting in rapid iron oxidation, reduced mixing and ultimately a reduced arsenic removing performance. Additionally it would result in rapid localized clogging of the system requiring frequent backwashing.

It is hypothesised that the aforementioned short-circuiting effects can be limited when multiple electrode bundles (anode and cathode sets) are placed in series in the filter bed (see Appendix 4 for graphical overview). Each of the bundles would release a fraction of the total iron, with the idea that the iron would be spread more uniform over the bed and mixing is enhanced. More uniform iron concentrations over the bed would enhance the arsenic removal efficiency of the system (paragraph 4.1). These bundles should however be placed some distance away from each other to prevent rapid iron oxidation and precipitate formation near the downstream cathode. This rapid formation of precipitates will likely result in rapid clogging and an additional increase in resistance of the electrochemical cells (and so the energy consumption) as precipitates will be retained in the cell. Experiments will have to be executed to confirm the hypothesis and show the added value of this design.

A system with a high removal efficiency, such as the integrated system with the electrodes in the filter bed, required low amounts of iron to be dosed. Reducing the required iron dosage significantly reduces the energy consumption, minimizes clogging of the filter bed and also reduces the waste sludge production (paragraph 4.2). Despite the increased arsenic removal for the integrated electrodes it can be doubted whether integrating the electrodes in the filter bed is an optimal solution to enhance arsenic removal. As observed, a higher energy consumption and an increase in energy consumption over time were undesired system properties of the electrodes in the filter bed compared to placing electrodes in the supernatant. Additionally, the partly homogeneous release of iron over the filter bed and the occurrence of non-uniform iron concentrations in the filter bed resulted in non-optimal arsenic removal conditions. Ideally the electrodes would be vertically placed in a bulk solution to avoid the accumulation of precipitates (with its undesired side effects), with As(III) oxidation prior to the Fe-EC treatment. If a floating bio-carrier (such as pall rings) would be implemented in the supernatant of a sand filter, on which AsOB can grow, the influent As(III) will be oxidized to As(V) prior to passing the electrodes. These bio-carriers will provide the desired oxidation of As(III) prior to Fe-EC treatment and ensure a high arsenic removal efficiency. The drawback of implementing these bio-carriers is the low A/V-ratio (area to volume) of the floating bio-carriers available in the market, resulting in insufficient AsOB biomass growth and arsenic oxidation. A bio-carrier with a high A/V-ratio and where naturally present iron precipitates do not cause clogging and/or block of the pores would be critical for this design to work.

4.5 Practical implementation and limitations

When considering a technology for practical implementation, scalability of the system is an urgent design question. Using the current setup/design, the system produced around 13 L/h of water that can be considered as water with arsenic concentrations below the WHO guideline after optimization of certain operating parameters. The design of a single electrode and cathode placed in the filter bed is very suitable for small decentralized systems with a low daily water production, as in addition to the current filter setup only a DC power source and steel electrodes are needed to operate the system at a high efficiency. The drawback of the system is the time needed to establish the AsOB (9 weeks in this study), meaning the system cannot be operated directly after installation and requires proper monitoring to track the As(III) oxidation. For the design of new RSF in decentralized areas it could be beneficial to have 2 separate filters, where the first one provides the As(III) oxidation and the second one has the Fe-EC in the supernatant followed by the removal of iron by the second filter bed. This design does not require to place the electrodes during backwashing, which improves the ease of operation. Upscaling the existing design for larger RSF will require a phase of redesign and testing, as the current design with the small electrodes connected by a simple fishing wire and crocodile clamps is fragile and will not work for large/heavy systems. It is expected that there is a maximum plate dimension to provide a (semi) homogeneous iron release over the filter bed, which will require to install multiple smaller electrodes (and connections to a DC power source) over the surface of larger filters. For large RSF setup, a framework and supporting structure will need to be designed to carry the electrodes and to get the current from the DC power source to the electrodes. The design of a large scale implementation could look something like the design presented in Appendix 4. Further research and flowthrough experiments applying this large scale implementation will need to be executed to provide insights in design and operation.

The water matrix used in these experiments did not have similar characteristics as raw groundwater, that commonly contains (high levels of) other contaminants, like phosphate, ammonium/nitrate, natural organic matter (NOM)/Humic acid (HA), silica, manganese, calcium and iron. This lack of groundwater characteristics makes it impossible to directly translate the system's performance to operation in the field, as it is well known that these aforementioned contaminants will affect the arsenic removal efficiency and the formation of passivation layers on the electrodes. For example, the presence of phosphate is known to reduce the arsenic removal efficiency related to competition between arsenic and phosphate for adsorption on the iron precipitates (van Genuchten et al., 2012; Dixit & Hering, 2003; Lakshmanan et al., 2010). Additionally, the presence of phosphate promotes the formation of passivation layers resulting in a reduced FE and an increasing energy consumption for a stable iron release (Müller et al., 2019; van Genuchten et al., 2017). Another contaminant affecting the arsenic removal is NOM/HA, as other studies found that the presence of NOM reduced the arsenic adsorption to iron precipitates/flocks (Banerji & Chaudhari, 2016; Tong et al., 2014). Literature shows that Sulphate (SO_4^{2-}) and Nitrate (NO_3^-) do not affect the arsenic removal efficiency and Fe:As ratios (Banerji & Chaudhari, 2016; Wan et al., 2011), however these contaminants promote the formation of passivation layers and reduced the FE and so the iron release of the systems (van Genuchten et al., 2017). For calcium it is known that it's presence increases arsenic removal efficiencies (van Genuchten et al., 2014), the drawback of the presence of calcium is scale ($CaCO_3$) formation on the electrodes (Van Genuchten et al., 2016).

Concentrations of adsorbed arsenic to HFO have not been considered in this study as it was assumed that this arsenic would be removed by a sand layer (with small grain size) with sufficient thickness. For the fully integrated experiments with As(III) and AsOB, 9 and 3 µg/L of arsenic adsorbed to HFO was found in the effluent of the experiments with the electrodes in the filter bed and supernatant respectively. This difference was caused by the thickness of anthracite below the electrodes in the filter bed and supernatant, as a higher filter bed (30 and 80 cm anthracite respectively) resulted in a higher removal of iron (0.1 and 0.2 mg/L in the effluent). With less iron present, the concentration of arsenic adsorbed to HFO flocks was lower. Depth profiles showed that the 40 cm of anthracite below the anode removed approx. 1.2 mg/L of iron for both electrode configurations, indicating similar removal mechanisms. These results showed that for future design and implementation it is of major importance to ensure sufficient filtration of the iron precipitates as the removal of iron proves to be important to achieve arsenic drinking water guidelines.

An undiscussed aspect of the long term increase in energy consumption is a perspective on aging of the electrodes (and especially the anode), affecting the long term operation of these systems. This effect can be shown when comparing the increase in energy consumption between a new and a previously used electrode (used for 12 operating cycles of 7 hours operated at 0.023 A). With a similar initial energy consumption, an increase in energy consumption (after treating 100L of water) of 96% (+0.013 kWh/m^3) and 19% (+0.003 kWh/m^3) was observed for the previously used electrode and new electrode respectively. One-way Anova showed that the differences in increasing energy consumption were significantly different ($p < 0.05$). Both electrodes were cleaned according the same procedure using sand paper and kept in acid overnight, for both electrodes the initial energy consumption was similar. It is hypothesised that the differences over time are caused by the smoothness of the surface, related to the effects of pitting corrosion. Observations showed that the occurrence of pitting corrosion created small holes in the surface, which made the surface of the electrode less smooth (Fig. 27). With a less smooth surface regarding the previously used electrode, dead zones were more likely to occur at the surface. These dead zones prevented the transport of iron away from the electrode's surface, promoting the accumulation of iron precipitates and increasing the cell resistance. Follow up experiments, focussing on long term effects, must be executed to characterize and validate the formation of surface layers and elaborate on processes that increase the resistance of the cell over time.

Fig. 27: Comparison of the surface on the top of the anode for the integrated electrodes. New anode (left) and previously used anode (right) with clear differences in smoothness of the surface caused by pitting corrosion.

As this study did not focus on the long term performance and iron release of the system and electrodes, the formation of passivation layers has not been investigated in detail. When focussing on the long term operation, the removal of the passivation layers from the anode (and cathode) would be of importance to counter the decrease in Faradaic efficiency (to << 1) (Müller et al., 2019; van Genuchten et al., 2017). When the FE decreases, a higher current has to be applied to ensure the released iron concentration is not affected (eq. 5 and 6), resulting in a higher energy consumption (eq. 7). Cleaning the electrodes with steel brushes or sand paper removes these passivation layers, requiring proper operation and maintenance of such systems (Amrose et al., 2014). It is hypothesised that backwashing of the system with the electrodes still in or just above the filter bed has the ability to remove part of the surface layers by sand grains scratching the surface of the electrodes. This behaviour has however not been investigated in this study, as at the end of the day the electrodes were removed after backwashing and cleaned with sand paper and acid. The effect of backwashing on the electrodes could be an interesting research topic for long term studies focussing on similar system design.

The next step for this technology should focus on the comparison between iron dosage and energy consumption for the different electrode configurations (in supernatant and in filter bed) when similar effluent arsenic concentrations of < 10 µg/L are reached when treating natural groundwater. This would provide decisive insights on the performance evaluation related to the effect of higher operating voltages, increasing voltage over time and required iron dosage (CD).

5. Conclusions and recommendations

In this study it was investigated whether integrating iron electrocoagulation (Fe-EC) within a biologically active filter bed could improve arsenic removal. Using the arsenic oxidizing bacteria (AsOB), naturally present in rapid sand filters (RSF), efficient As(III) oxidation could be achieved without using any chemicals. As proven in earlier studies, the oxidation of As(III) prior to Fe-EC treatment would significantly increase the arsenic removal efficiency. The idea was to design a system where As(III) was oxidized to As(V) prior to the treatment with Fe-EC and could easily be integrated within existing RSF. Electrodes were embedded in the filter bed as horizontally placed perforated plates, which were placed in and taken out the filter bed during backwashing.

As(V) experiments showed the effect of pH, flowrate and increased charge dosage (CD) on arsenic removal efficiency for electrodes integrated in the filter bed. By taking out the biological oxidation part from the system, the performance and behaviour of the electrodes in the filter bed could be assessed separately. As(V) removal was enhanced by reducing the pH from 8 to 7 and by increasing the CD (iron dosage). Most importantly, these experiments showed rising drawbacks, like the increasing energy consumption over time and reduced arsenic removal efficiency when placing the electrodes in the filter bed. The reduced arsenic removal proved to be a consequence of a partial homogeneous iron release by the electrodes and improper mixing in the filter bed. These two aspects caused non-uniform concentrations of iron that was generated at the electrodes and short-circuiting of flows, causing the reduced arsenic removal efficiency.

Experiments regarding the growth of AsOB and the As(III) oxidation profile showed that backwashing affected the oxidation pattern after the initial backwash, but during the remaining experiments this effect proved to be neglectable. These results imply that biological arsenic oxidation by AsOB in RSF provide consistent and reliable As(III) oxidation during daily operation. Additionally it was shown that the arsenic removal from 150 to 50 µg/L is more efficient in a system with the Fe-EC placed in the supernatant of a RSF with AsOB (Fe:As of 18.3, for a CD of 6.4 C/L) than in previously executed batch experiments with Fe-EC alone (Fe:As of 116, for a CD of 20 C/L). Despite the reduced arsenic removal efficiency for electrodes in the filter bed, the Fe:As ratio went from 18.3 to 15.0 (removal from 49 to 29 µg/L in the effluent from an initial 150 µg/L As(III)) when placing the electrodes in the filter bed with AsOB instead of in the supernatant. These results for similar operating conditions (CD of 6.4 C/L, pH of 8.0 and a flowrate of 3 m/h) proved that the arsenic removal performance can indeed be enhanced by introducing the iron after the biological oxidation. However, the downside of placing the electrodes in the filter bed is the increase in operating voltage from 4.1 to 8.1 V and the corresponding increase in energy consumption (from 0.007 to 0.014 kWh/m^3). Additionally, the electrodes in the filter bed showed a rising energy consumption during the treatment of 100L of water (+0.003 kWh/m^3) while for the electrodes in the supernatant this trend was not observed.

These experiments showed that besides arsenic removal efficiency, operational parameters such as iron dosage, energy consumption, sludge production, and clogging are relevant when implementing (new) technologies. Even though the electrodes placed in the filter bed with AsOB removed more arsenic, a higher energy consumption, improper mixing and short-circuiting of flows indicated that the performance can be further optimized. Optimization of the design and new

approaches that could overcome these drawbacks are proposed, urging the need for a research focus on implementing novel technologies in flowthrough systems. Flowthrough experiments will provide valuable practical insights in the advantages and disadvantages of new technologies, showing the way forward to bring the science of arsenic removal closer to practice.

References

Amrose, S. E., Bandaru, S. R. S., Delaire, C., Van Genuchten, C. M., Dutta, A., DebSarkar, A., Orr, C., Roy, J., Das, A., & Gadgil, A. J. (2014). Electro-chemical arsenic remediation: Field trials in West Bengal. *Science of The Total Environment, 488–489*, 539–546. https://doi.org/10.1016/j.scitotenv.2013.11.074

Amrose, S., Gadgil, A., Srinivasan, V., Kowolik, K., Muller, M., Huang, J., & Kostecki, R. (2013). Arsenic removal from groundwater using iron electrocoagulation: Effect of charge dosage rate. *Journal of Environmental Science and Health, Part A, 48*(9), 1019–1030. https://doi.org/10.1080/10934529.2013.773215

Annaduzzaman, M., Rietveld, L. C., Hoque, B. A., Bari, M. N., & van Halem, D. (2021). Arsenic removal from iron-containing groundwater by delayed aeration in dual-media sand filters. *Journal of Hazardous Materials, 411*, 124823. https://doi.org/10.1016/j.jhazmat.2020.124823

Argos, M., Kalra, T., Rathouz, P. J., Chen, Y., Pierce, B., Parvez, F., Islam, T., Ahmed, A., Rakibuz-Zaman, M., Hasan, R., Sarwar, G., Slavkovich, V., van Geen, A., Graziano, J., & Ahsan, H. (2010). Arsenic exposure from drinking water, and all-cause and chronic-disease mortalities in Bangladesh (HEALS): a prospective cohort study. *The Lancet, 376*(9737), 252–258. https://doi.org/10.1016/s0140-6736(10)60481-3

Banerji, T., & Chaudhari, S. (2016). Arsenic removal from drinking water by electrocoagulation using iron electrodes- an understanding of the process parameters. *Journal of Environmental Chemical Engineering, 4*(4), 3990–4000. https://doi.org/10.1016/j.jece.2016.09.007

Bissen, M., & Frimmel, F. H. (2003). Arsenic— a Review. Part II: Oxidation of Arsenic and its Removal in Water Treatment. *Acta hydrochimica et hydrobiologica, 31*(2), 97–107. https://doi.org/10.1002/aheh.200300485

Bruins, J. H., Vries, D., Petrusevski, B., Slokar, Y. M., & Kennedy, M. D. (2013). Assessment of manganese removal from over 100 groundwater treatment plants. *Journal of Water Supply: Research and Technology-Aqua, 63*(4), 268–280. https://doi.org/10.2166/aqua.2013.086

Cavalca, L., Corsini, A., Zaccheo, P., Andreoni, V., & Muyzer, G. (2013). Microbial transformations of arsenic: perspectives for biological removal of arsenic from water. *Future Microbiology, 8*(6), 753–768. https://doi.org/10.2217/fmb.13.38

Chen, D., Yen, M., Lin, P., Groff, S., Lampo, R., McInerney, M., & Ryan, J. (2014). A Corrosion Sensor for Monitoring the Early-Stage Environmental Corrosion of A36 Carbon Steel. *Materials, 7*(8), 5746–5760. https://doi.org/10.3390/ma7085746

Delaire, C., Amrose, S., Zhang, M., Hake, J., & Gadgil, A. (2017). How do operating conditions affect As(III) removal by iron electrocoagulation? *Water Research, 112*, 185–194. https://doi.org/10.1016/j.watres.2017.01.030

Dixit, S., & Hering, J. G. (2003). Comparison of Arsenic(V) and Arsenic(III) Sorption onto Iron Oxide Minerals: Implications for Arsenic Mobility. *Environmental Science & Technology, 37*(18), 4182–4189. https://doi.org/10.1021/es030309t

Flores, O. J., Nava, J. L., Carreño, G., Elorza, E., & Martínez, F. (2013). Arsenic removal from groundwater by electrocoagulation in a pre-pilot-scale continuous filter press reactor. *Chemical Engineering Science, 97*, 1–6. https://doi.org/10.1016/j.ces.2013.04.029

Ghurye, G., & Clifford, D. (2004). As(III) oxidation using chemical and solid-phase oxidants. *Journal - American Water Works Association, 96*(1), 84–96. https://doi.org/10.1002/j.1551-8833.2004.tb10536.x

Goren, A., Kobya, M., & Oncel, M. (2020). Arsenite removal from groundwater by aerated electrocoagulation reactor with Al ball electrodes: Human health risk assessment. *Chemosphere, 251*, 126363. https://doi.org/10.1016/j.chemosphere.2020.126363

Gude, J. C. J., Joris, K., Huysman, K., Rietveld, L. C., & van Halem, D. (2018a). Effect of supernatant water level on As removal in biological rapid sand filters. *Water Research X, 1*, 100013. https://doi.org/10.1016/j.wroa.2018.100013

Gude, J. C. J., Rietveld, L. C., & van Halem, D. (2018b). As(III) removal in rapid filters: Effect of pH, Fe(II)/Fe(III), filtration velocity and media size. *Water Research, 147*, 342–349. https://doi.org/10.1016/j.watres.2018.10.005

Gude, J. C. J., Rietveld, L. C., & van Halem, D. (2018c). Biological As(III) oxidation in rapid sand filters. *Journal of Water Process Engineering, 21*, 107–115. https://doi.org/10.1016/j.jwpe.2017.12.003

Hove, M., Van Hille, R. P., & Lewis, A. E. (2008). Mechanisms of formation of iron precipitates from ferrous solutions at high and low pH. *Chemical Engineering Science, 63*(6), 1626–1635. https://doi.org/10.1016/j.ces.2007.11.016

Hug, S. J., & Leupin, O. (2003). Iron-Catalyzed Oxidation of Arsenic(III) by Oxygen and by Hydrogen Peroxide: pH-Dependent Formation of Oxidants in the Fenton Reaction. *Environmental Science & Technology, 37*(12), 2734–2742. https://doi.org/10.1021/es026208x

Kapaj, S., Peterson, H., Liber, K., & Bhattacharya, P. (2006). Human Health Effects From Chronic Arsenic Poisoning–A Review. *Journal of Environmental Science and Health, Part A, 41*(10), 2399–2428. https://doi.org/10.1080/10934520600873571

Katsoyiannis, I. A., Ruettimann, T., & Hug, S. J. (2008a). pH Dependence of Fenton Reagent Generation and As(III) Oxidation and Removal by Corrosion of Zero Valent Iron in Aerated Water. *Environmental Science & Technology, 42*(19), 7424–7430. https://doi.org/10.1021/es800649p

Katsoyiannis, I. A., Zikoudi, A., & Hug, S. J. (2008b). Arsenic removal from groundwaters containing iron, ammonium, manganese and phosphate: A case study from a treatment unit in northern Greece. *Desalination, 224*(1–3), 330–339. https://doi.org/10.1016/j.desal.2007.06.014

Kinniburgh, D. G., & Smedley, P. (2001). Arsenic contamination of groundwater in Bangladesh. Keyworth, U.K.: *British Geological Survey, vol. 1–4*

Kobya, M., Demirbas, E., & Ulu, F. (2016). Evaluation of operating parameters with respect to charge loading on the removal efficiency of arsenic from potable water by electrocoagulation. *Journal of Environmental Chemical Engineering, 4*(2), 1484–1494. https://doi.org/10.1016/j.jece.2016.02.016

Kobya, M., Gebologlu, U., Ulu, F., Oncel, S., & Demirbas, E. (2011). Removal of arsenic from drinking water by the electrocoagulation using Fe and Al electrodes. *Electrochimica Acta, 56*(14), 5060–5070. https://doi.org/10.1016/j.electacta.2011.03.086

Lakshmanan, D., Clifford, D. A., & Samanta, G. (2010). Comparative study of arsenic removal by iron using electrocoagulation and chemical coagulation. *Water Research, 44*(19), 5641–5652. https://doi.org/10.1016/j.watres.2010.06.018

Lee, C. O., Boe-Hansen, R., Musovic, S., Smets, B., Albrechtsen, H. J., & Binning, P. (2014). Effects of dynamic operating conditions on nitrification in biological rapid sand filters for drinking water treatment. *Water Research, 64*, 226–236. https://doi.org/10.1016/j.watres.2014.07.001

Li, L., van Genuchten, C. M., Addy, S. E. A., Yao, J., Gao, N., & Gadgil, A. J. (2012). Modeling As(III) Oxidation and Removal with Iron Electrocoagulation in Groundwater. *Environmental Science & Technology, 46*(21), 12038–12045. https://doi.org/10.1021/es302456b

Martínez-Villafañe, J., Montero-Ocampo, C., & García-Lara, A. (2009). Energy and electrode consumption analysis of electrocoagulation for the removal of arsenic from underground water. *Journal of Hazardous Materials, 172*(2–3), 1617–1622. https://doi.org/10.1016/j.jhazmat.2009.08.044

Mollah, M., Morkovsky, P., Gomes, J., Kesmez, M., Parga, J., & Cocke, D. (2004). Fundamentals, present and future perspectives of electrocoagulation. *Journal of Hazardous Materials, 114*(1–3), 199–210. https://doi.org/10.1016/j.jhazmat.2004.08.009

Müller, S., Behrends, T., & van Genuchten, C. M. (2019). Sustaining efficient production of aqueous iron during repeated operation of Fe(0)-electrocoagulation. *Water Research, 155*, 455–464. https://doi.org/10.1016/j.watres.2018.11.060

Nicomel, N., Leus, K., Folens, K., Van Der Voort, P., & Du Laing, G. (2015). Technologies for Arsenic Removal from Water: Current Status and Future Perspectives. *International Journal of Environmental Research and Public Health, 13*(1), 62. https://doi.org/10.3390/ijerph13010062

Podgorski, J., & Berg, M. (2020). Global threat of arsenic in groundwater. Science, 368(6493), 845–850. https://doi.org/10.1126/science.aba1510

Roberts, L. C., Hug, S. J., Ruettimann, T., Billah, M. M., Khan, A. W., & Rahman, M. T. (2004). Arsenic Removal with Iron(II) and Iron(III) in Waters with High Silicate and Phosphate Concentrations. *Environmental Science & Technology, 38*(1), 307–315. https://doi.org/10.1021/es0343205

Roh, T., Lynch, C. F., Weyer, P., Wang, K., Kelly, K. M., & Ludewig, G. (2017). Low-level arsenic exposure from drinking water is associated with prostate cancer in Iowa. *Environmental research, 159*, 338–343. https://doi.org/10.1016/j.envres.2017.08.026

Roy, M., van Genuchten, C. M., Rietveld, L., & van Halem, D. (2021). Integrating biological As(III) oxidation with Fe(0) electrocoagulation for arsenic removal from groundwater. *Water Research, 188*, 116531. https://doi.org/10.1016/j.watres.2020.116531

Saint-Jacques, N., Brown, P., Nauta, L., Boxall, J., Parker, L., & Dummer, T. J. (2018). Estimating the risk of bladder and kidney cancer from exposure to low-levels of arsenic in drinking water, Nova Scotia, Canada. *Environment International, 110*, 95–104. https://doi.org/10.1016/j.envint.2017.10.014

Schwertmann, U., & Cornell, R. M. (2000). *Iron Oxides in the Laboratory: Preparation and Characterization* (2nd ed.). Wiley-VCH.

Sharma, S. K., Kappelhof, J., Groenendijk, M., Schippers, J. C., & Schippers, J. C. (2001). Comparison of physicochemical iron removal mechanisms in filters. *Journal of Water Supply: Research and Technology-Aqua, 50*(4), 187–198. https://doi.org/10.2166/aqua.2001.0017

Sodhi, K. K., Kumar, M., Agrawal, P. K., & Singh, D. K. (2019). Perspectives on arsenic toxicity, carcinogenicity and its systemic remediation strategies. *Environmental Technology & Innovation, 16*, 100462. https://doi.org/10.1016/j.eti.2019.100462

Song, P., Yang, Z., Zeng, G., Yang, X., Xu, H., Wang, L., Xu, R., Xiong, W., & Ahmad, K. (2017). Electrocoagulation treatment of arsenic in wastewaters: A comprehensive review. *Chemical Engineering Journal, 317*, 707–725. https://doi.org/10.1016/j.cej.2017.02.086

Spijker, J. (2008). Arseen in Nederlands grondwater. Oorzaak verhoogde arseenconcentraties. *RIVM briefrapport 607300009*/2008.

Steinmaus, C., Ferreccio, C., Acevedo, J., Yuan, Y., Liaw, J., Durán, V., Cuevas, S., García, J., Meza, R., Valdés, R., Valdés, G., Benítez, H., VanderLinde, V., Villagra, V., Cantor, K. P., Moore, L. E., Perez, S. G., Steinmaus, S., & Smith, A. H. (2014). Increased Lung and Bladder Cancer Incidence in Adults after In Utero and Early-Life Arsenic Exposure. *Cancer Epidemiology Biomarkers & Prevention, 23*(8), 1529–1538. https://doi.org/10.1158/1055-9965.epi-14-0059

Stuijfzand, P. J., van Rossum, P., & Mendizabal, I. (2008). Does arsenic, in groundwaters of the compound Rhine-Meuse-Scheldt-Ems delta, menace drinking water supply in the Netherlands? In Appelo (Ed.), *Proceedings IAH Conference*. Arsenic in groundwater, a world problem, 102–125

Tong, M., Yuan, S., Zhang, P., Liao, P., Alshawabkeh, A. N., Xie, X., & Wang, Y. (2014). Electrochemically Induced Oxidative Precipitation of Fe(II) for As(III) Oxidation and Removal in Synthetic Groundwater. *Environmental Science & Technology, 48*(9), 5145–5153. https://doi.org/10.1021/es500409m

van der Wens, P., Baken, K., & Schriks, M. (2016). Arsenic at low concentrations in Dutch drinking water: Assessment of removal costs and health benefits. *Arsenic in the Environment - Proceedings*, 563–564. https://doi.org/10.1201/b20466-262

van Genuchten, C. M., Addy, S. E. A., Peña, J., & Gadgil, A. J. (2012). Removing Arsenic from Synthetic Groundwater with Iron Electrocoagulation: An Fe and As K-Edge EXAFS Study. *Environmental Science & Technology, 46*(2), 986–994. https://doi.org/10.1021/es201913a

van Genuchten, C. M., Bandaru, S. R., Surorova, E., Amrose, S. E., Gadgil, A. J., & Peña, J. (2016). Formation of macroscopic surface layers on Fe(0) electrocoagulation electrodes during an extended field trial of arsenic treatment. *Chemosphere, 153*, 270–279. https://doi.org/10.1016/j.chemosphere.2016.03.027

van Genuchten, C. M., Behrends, T., Kraal, P., Stipp, S., & Dideriksen, K. (2018). Controls on the formation of Fe(II,III) (hydr)oxides by Fe(0) electrolysis. *Electrochimica Acta, 286*, 324–338. https://doi.org/10.1016/j.electacta.2018.08.031

van Genuchten, C. M., Behrends, T., Stipp, S., & Dideriksen, K. (2020). Achieving arsenic concentrations of <1 µg/L by Fe(0) electrolysis: The exceptional performance of magnetite. *Water Research, 168*, 115170. https://doi.org/10.1016/j.watres.2019.115170

van Genuchten, C. M., Dalby, K., Ceccato, M., Stipp, S., & Dideriksen, K. (2017). Factors affecting the Faradaic efficiency of Fe(0) electrocoagulation. *Journal of Environmental Chemical Engineering, 5*(5), 4958–4968. https://doi.org/10.1016/j.jece.2017.09.008

van Genuchten, C. M., Peña, J., Amrose, S. E., & Gadgil, A. J. (2014). Structure of Fe(III) precipitates generated by the electrolytic dissolution of Fe(0) in the presence of groundwater ions. *Geochimica et Cosmochimica Acta, 127*, 285–304. https://doi.org/10.1016/j.gca.2013.11.044

van Halem, D., Bakker, S. A., Amy, G. L., & van Dijk, J. C. (2009). Arsenic in drinking water: a worldwide water quality concern for water supply companies. *Drinking Water Engineering and Science, 2*(1), 29–34. https://doi.org/10.5194/dwes-2-29-2009

Verruijt, A., 2001, 2012. *Soil Mechanics*. Delft University of Technology – Vssd

Wan, W., Pepping, T. J., Banerji, T., Chaudhari, S., & Giammar, D. E. (2011). Effects of water chemistry on arsenic removal from drinking water by electrocoagulation. *Water Research, 45*(1), 384–392. https://doi.org/10.1016/j.watres.2010.08.016

World Health Organization, WHO. (2004). Guidelines For Drinking-Water Quality, vol. 1. Recommendations, 3rd ed World Health Organization, Geneva, Switzerland.

Yang, L., Li, X., Chu, Z., Ren, Y., & Zhang, J. (2014). Distribution and genetic diversity of the microorganisms in the biofilter for the simultaneous removal of arsenic, iron and manganese from simulated groundwater. *Bioresource Technology, 156*, 384–388. https://doi.org/10.1016/j.biortech.2014.01.067

Supplementary information

Appendix 1; Electrode characteristics

Geperforeerd Staal
Dikte: 2 mm.
Materiaal : STW22
: Werkstofnummer 1.0332
: Warmgewalst
Chem.samenstelling
(richtwaarde) (target): : C : 0,10% max. %
: Si : 0,15% max. %
: P : max. 0,035 %
: S : max. 0,035 %
: Mn : max. 0,035 %
: N : max. 0,007 %

Mechanische eigenschappen
Soortelijk gewicht : 7,85

Diameter Anode: 75 mm
Diameter Cathode: 55 mm

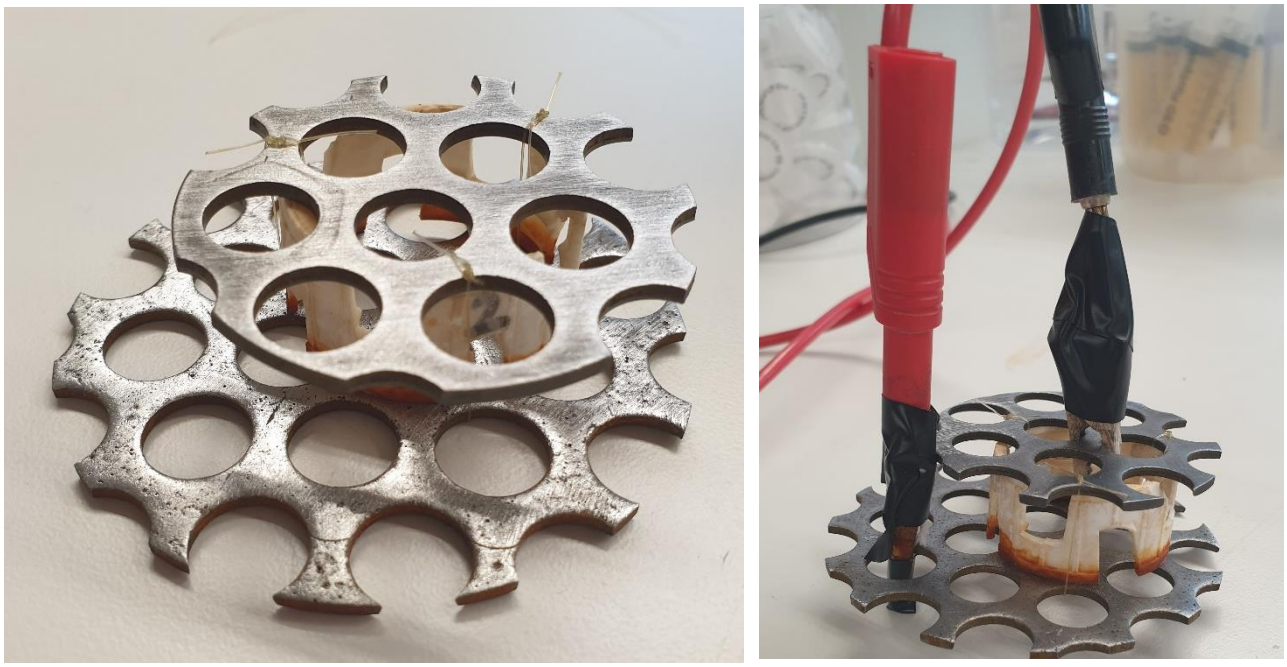

Fig. S1: Anode and cathode configuration (left) and connection of the electrodes to the DC power source (right). In this configuration the cathode anode can be seen on top of the anode, connected by nylon wire and a plastic spacer in between.

Appendix 2; Tap water characteristics

Table with water characteristics (Roy et al., 2021)

Table S1: Tap water composition

Ion	Initial value
pH	7.0-8.0
PO_4^{3-}	0
SO_4^{2-}	52.1 ± 0.98 mg/L
NO_2^-	0
NO_3^-	2.39 ± 0.31 mg/L
NH_4^+	0
Fe	0
As	0
Ca^{2+}	49.76 ± 0.3 mg/L
Na^+	41.50 ± 0.42 mg/L
Si	2.15 ± 0.04 mg/L
Mg^{2+}	6.95 ± 0.09 mg/L

Appendix 3; Porosity and particle size distribution

The porosity of the sand and anthracite was estimated by filling a graduated cylinder (VWR 250:2 plastic cylinder), with a total volume of 250 mL, with 120 to 140 mL of demi water. Next, a substantial amount of the dried sand/anthracite (65-110 mL) was carefully poured into the cylinder to avoid entrapment of air bubbles within the granular layer. During and after the addition of the material to the graduated cylinder, the cylinder was firmly tapped to ensure the sand/anthracite would settle. After compaction, the added volume of the granular layer and the volume of the water layer on top was reported. The experiment was repeated 5 times, using equation S1 (Verruijt, 2001) the porosity was estimated.

$$porosity_{soil} = \frac{Volume_{pores}}{Volume_{soil}} \quad \text{(S1)}$$

A sieving analysis, using a vibrating sieve tower, was used to determine the Particle Size Distribution (PSD) of the sand and anthracite. Sieves with a 4, 3.35, 2.3, 1.8, 1.7, 1.6, 1.4, 1.18, 0.85, 0.6, 0.5, 0.425, 0.3 mm opening were used. Fig. S2 gives the results of the PSD for both materials.

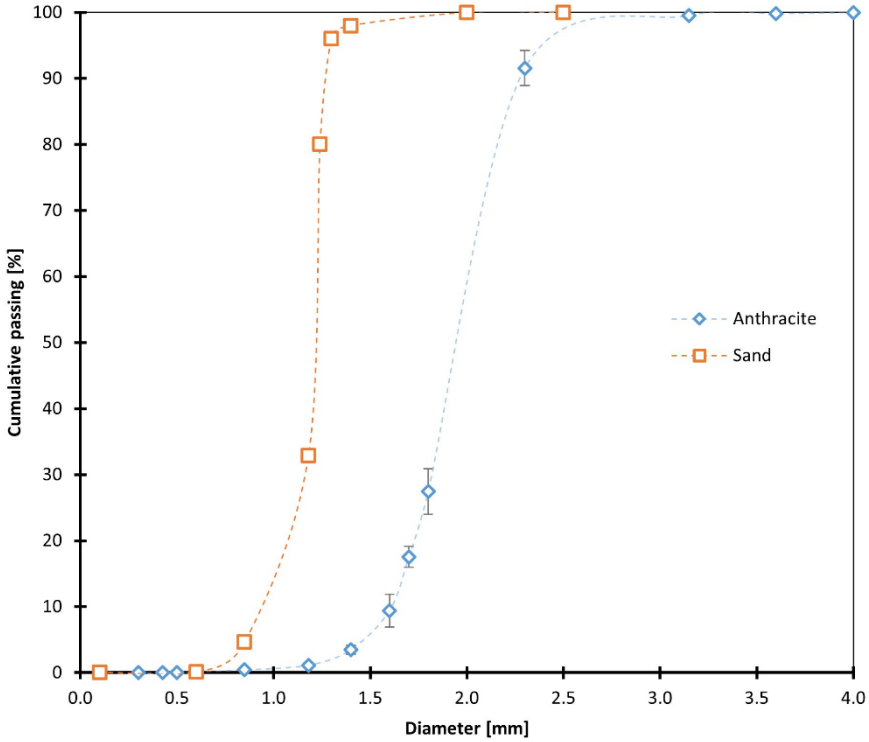

Fig. S2: Particle size distribution of used sand and anthracite. Error bars represent min and max values of duplicates.

Appendix 4; Overview of suggestions for system improvement and scalability

The overview below gives a graphical presentation of the proposed system redesign with multiple electrode bundles installed in series embedded in the anthracite (Fig. S3). Each electrode bundle (anode + cathode) has its own connection to a DC power source, that provides the desired current to each bundle.

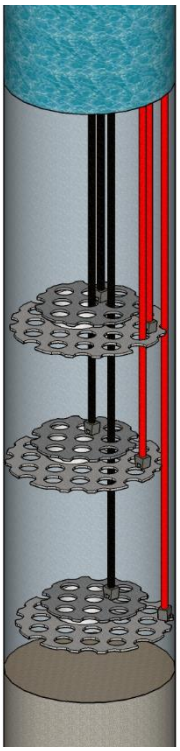

Fig. S3: Fully integrated system design with multiple electrode bundles in series embedded in anthracite layer.

Fig. S4 gives a graphical overview of an example of a scaled version of the original design. Multiple electrode bundles (anode + cathode) have been installed with their own connection to a DC power source. The electrode bundles have been positioned next to each other in such a way that the entire surface (plane) of the RSF is covered with electrodes, with the aim to ensure a (partly) homogeneous release of iron.

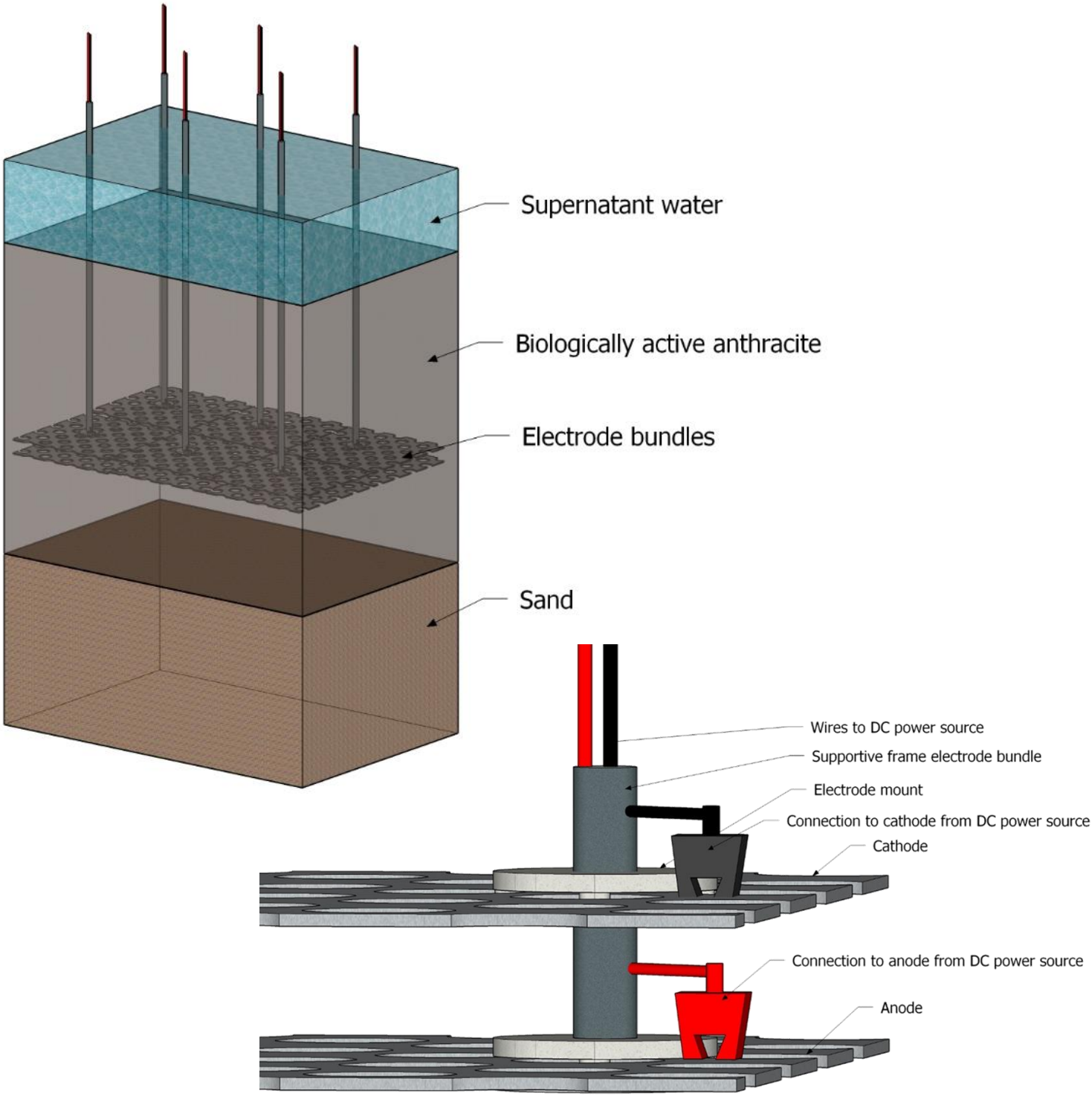

Fig. S4: Overview of scaled system with supporting framework (top left) and detailed view of connections of a single part of the framework (bottom right)